



Contents lists available at ScienceDirect

Physics Letters B

www.elsevier.com/locate/physletb



Search for invisible Higgs boson decays in vector boson fusion at $\sqrt{s} = 13$ TeV with the ATLAS detector

The ATLAS Collaboration ^{*}

ARTICLE INFO

Article history:

Received 18 September 2018
 Received in revised form 12 February 2019
 Accepted 9 April 2019
 Available online xxxx
 Editor: M. Doser

ABSTRACT

We report a search for Higgs bosons that are produced via vector boson fusion and subsequently decay into invisible particles. The experimental signature is an energetic jet pair with invariant mass of $\mathcal{O}(1)$ TeV and $\mathcal{O}(100)$ GeV missing transverse momentum. The analysis uses 36.1 fb^{-1} of pp collision data at $\sqrt{s} = 13 \text{ TeV}$ recorded by the ATLAS detector at the LHC. In the signal region the 2252 observed events are consistent with the background estimation. Assuming a 125 GeV scalar particle with Standard Model cross sections, the upper limit on the branching fraction of the Higgs boson decay into invisible particles is 0.37 at 95% confidence level where 0.28 was expected. This limit is interpreted in Higgs portal models to set bounds on the WIMP–nucleon scattering cross section. We also consider invisible decays of additional scalar bosons with masses up to 3 TeV for which the upper limits on the cross section times branching fraction are in the range of 0.3–1.7 pb.

© 2019 The Author(s). Published by Elsevier B.V. This is an open access article under the CC BY license (<http://creativecommons.org/licenses/by/4.0/>). Funded by SCOAP³.

1. Introduction

We present a search for the decays of the Higgs boson [1,2], produced via the vector boson fusion (VBF) process [3,4], into invisible particles ($\chi\bar{\chi}$) with an anomalous and sizable $\mathcal{O}(10)\%$ branching fraction. The hypothesis under consideration [5–16] is that the Higgs boson might decay into a pair of weakly interacting massive particles (WIMP) [17,18], which may explain the nature of dark matter (see Ref. [19] and the references therein). The search carried out for the 125 GeV Higgs boson is repeated for hypothetical scalars with masses up to 3 TeV. The search is independent on the decay of the mediator because the final state particles are invisible to the detector, while it is dependent on its $E_{\text{T}}^{\text{miss}}$ distribution (defined below) because that quantity is reflective of the mediator's p_{T} distribution.

The data sample corresponds to an integrated luminosity of 36.1 fb^{-1} of proton–proton (pp) collisions at $\sqrt{s} = 13 \text{ TeV}$ recorded by the ATLAS detector at the LHC in 2015 and 2016. The experimental signature of the VBF production process is a pair of energetic quark jets with a wide gap in pseudorapidity (η) corresponding to the $\mathcal{O}(1)$ TeV value of the invariant mass (m_{jj}) of the highest- p_{T} jets in the event.¹ The signature for the decay pro-

cess is the $\mathcal{O}(100)$ GeV value of the missing transverse momentum ($E_{\text{T}}^{\text{miss}}$) that corresponds to the Higgs boson p_{T} . The VBF topology offers a powerful rejection of the strongly produced² backgrounds due to single vector boson plus two jets, and the multijet background produced from QCD processes. In this analysis, the Higgs production via the gluon fusion mechanism is subdominant to VBF and is considered as part of the signal.

Direct searches for invisible Higgs decays look for an excess of events over Standard Model expectations. The absence of an excess is interpreted as an upper limit on the branching fraction of invisible decays (\mathcal{B}_{inv}) assuming the Standard Model production cross section [20] of the 125 GeV Higgs boson. Other published results have targeted a variety of production mechanisms—gluon fusion, VBF, W or Z associated production [21–25]—to set upper limits on \mathcal{B}_{inv} . The best limits are from the statistical combination of search results for which ATLAS reports an observed (expected) limit of 0.26 (0.17) [26] and CMS reports 0.26 (0.20) [27] at 95% confidence level (CL). For these combinations the single input with the highest expected sensitivity is VBF, the channel pursued here. For the VBF channel using Run-1 data, ATLAS reports 0.28 (0.31) [28] and CMS reports 0.43 (0.31) [29]. In a more recent update of the VBF channel using Run-2 data, ATLAS reports 0.37 (0.28) [this paper] CMS reports 0.33 (0.25) [27].

Global fits to the measurements of visible decay channels of the Higgs boson place indirect constraints on the beyond-the-SM

^{*} E-mail address: atlas.publications@cern.ch.

¹ ATLAS uses a right-handed coordinate system with its origin at the nominal interaction point in the center of the detector and the z -axis along the beam direction. The x -axis points from the interaction point to the center of the LHC ring; the y -axis points upward. Cylindrical coordinates (r, ϕ) are used in the transverse plane, where ϕ is the azimuthal angle around the z -axis. The pseudorapidity is defined as $\eta = -\ln(\tan(\theta/2))$, where θ is the polar angle.

² For the W and Z background processes in this paper, electroweak (EW) refers to diagrams that are of $\mathcal{O}(\alpha_{\text{EW}}^4)$ or greater, while strong refers to diagrams that are of $\mathcal{O}(\alpha_s^2)$ or greater accompanied by $\mathcal{O}(\alpha_{\text{EW}}^2)$.

<https://doi.org/10.1016/j.physletb.2019.04.024>

0370-2693/© 2019 The Author(s). Published by Elsevier B.V. This is an open access article under the CC BY license (<http://creativecommons.org/licenses/by/4.0/>). Funded by SCOAP³.

decay branching fraction \mathcal{B}_{BSM} . The \mathcal{B}_{BSM} is the sum of \mathcal{B}_{inv} that represents invisible decays and $\mathcal{B}_{\text{undet}}$ that represents the channels that are undetected, i.e., those that are not included in the following combination. For \mathcal{B}_{BSM} using Run-1 data, ATLAS reports 0.49 (0.48) [30] and CMS reports 0.57 (0.52) [31] with similar but not identical assumptions. A combination of ATLAS and CMS results using Run-1 data gives 0.34 (0.39) [32]. In a more recent update using Run-2 data, CMS reports an observed limit on $\mathcal{B}_{\text{undet}}$ of 0.38 [33]. As noted in Ref. [28], there is complementarity between the direct search for invisible Higgs decays and the indirect constraints from the global fits.

In this analysis, several changes and improvements are made with respect to the previous ATLAS paper on this topic [28]. The trigger and hadronic objects are defined considering the simultaneous pp collisions in the same and nearby bunch crossings (pileup) (Section 2). The leading backgrounds are simulated using state-of-the-art QCD predictions (Section 3). The event selections are changed to retain a good sensitivity despite the higher pileup. The analysis extracts the signal yield using a binned likelihood fit to the m_{jj} spectrum in 3 bins to increase the signal sensitivity (Section 4). The estimation of the important and dominant background for the $Z \rightarrow \nu\nu$ process (denoted $Z_{\nu\nu}$) relies only on the Z_{ee} and $Z_{\mu\mu}$ control samples, and is not affected by theoretical uncertainties of the W -to- Z extrapolation (Section 5). The systematic uncertainties are evaluated separately for each m_{jj} bin (Section 6). The search is repeated for other scalars with masses up to 3 TeV, which can easily be reinterpreted for models not considered in this Letter (Section 7). Several aspects of the analysis have not changed compared to the ATLAS Run-1 analysis—e.g., subdetector descriptions, transfer factor method, Higgs portal models—and details of these may be found in Ref. [28].

2. Detector, trigger, and analysis objects

ATLAS is a multipurpose particle physics detector with a forward-backward symmetric cylindrical geometry consisting of a tracking system, electromagnetic and hadronic calorimeters, and a muon system [34].

The trigger to record events in the sample containing the VBF signal candidates used a two-level $E_{\text{T}}^{\text{miss}}$ algorithm with thresholds adjusted throughout the data-taking period to cope with varying levels of pileup [35,36]. The LEVEL-1 system used coarse-granularity analog sums of the energy deposits in the calorimeter towers to require $E_{\text{T}}^{\text{miss}} > 50 \text{ GeV}$. The second-level HIGH LEVEL TRIGGER system [37] used jets that are reconstructed from calibrated clusters of cell energies [38] and requires $E_{\text{T}}^{\text{miss}} > 70$ –110 GeV depending on the luminosity and the pileup level. The trigger efficiency [39] for signal events is 98% for $E_{\text{T}}^{\text{miss}} > 180 \text{ GeV}$ when comparing the trigger selection with the offline $E_{\text{T}}^{\text{miss}}$ definition that contains additional corrections.

The triggers to record the control samples for background studies used lepton and jet algorithms [40]. The samples with leptonic W and Z decays were collected with a single-electron or -muon trigger with $p_{\text{T}} > 24 \text{ GeV}$ (26 GeV) and an isolation requirement in 2015 (towards the end of 2016). The sample of multijet events was collected using a set of low-threshold single-jet triggers with large prescale values to keep the event rate relatively low.

For each event, a vertex is reconstructed from two or more associated tracks (t) with $p_{\text{T}} > 400 \text{ MeV}$. If multiple vertices are present, we consider the one with the largest $\sum_t (p_{\text{T},t})^2$ as the primary vertex of our candidates.

Leptons ($\ell = e, \mu$) are identified to help characterize events with leptonic final states from decays of vector bosons. Since the signal process contains no leptons, such events are used for the background estimation, which is described in Section 5. Electrons

(muons) must have $p_{\text{T}} > 7 \text{ GeV}$, $|\eta| < 2.47$ (2.5), and satisfy an isolation requirement. Electrons are reconstructed by matching clustered energy deposits in the electromagnetic calorimeter to tracks from the inner detector [41,42] and muons by matching inner detector and muon spectrometer tracks [43]. For electrons (muons) with a p_{T} value of at least 30 GeV (20–100 GeV), the reconstruction efficiency 80% (96%) with a rejection factor of around 500 (600). All leptons must originate from the primary vertex.

Jets are reconstructed from topological clusters in the calorimeters using the anti- k_r algorithm [44] with a radius parameter $R = 0.4$. Jets must have $p_{\text{T}} > 20 \text{ GeV}$ and $|\eta| < 4.5$. The subset of jets with $p_{\text{T}} < 60 \text{ GeV}$ and $|\eta| < 2.4$ are jet vertex tagged (jvt) [45] to suppress pileup effects, using tracking and vertexing. The jvt is 92% efficient for the jets in the signal process from the primary interaction with a rejection factor of around 100 for pileup jets with p_{T} value in the range of 20–50 GeV [45].

Cleaning requirements help suppress non-collision backgrounds [46]. Fake jets due to noisy cells are removed by requiring a good fit to the expected pulse shape for each constituent calorimeter cell. Fake jets induced by beam-halo interactions with the LHC collimators are removed by requirements on their energy distribution and the fraction of their constituent tracks that originate from the primary vertex.

In events with identified leptons, an overlap removal procedure is applied to resolve the ambiguities in cases where a jet is also identified in the same η - ϕ area, which could occur in situations such as having a heavy-flavor hadron decay within a jet [47]. The lepton-jet overlap in ΔR distance³ is resolved sequentially as follows. If an electron is near a jet with $\Delta R < 0.2$, the jet is removed to avoid the double counting of electron energy deposits. If a remaining jet is near an electron with $0.2 \leq \Delta R < 0.4$, the electron is removed. If a muon is near a jet with $\Delta R < 0.4$ and the jet is associated with at least (less than) three charged tracks with $p_{\text{T}} > 500 \text{ MeV}$, the muon (jet) is removed.

The $E_{\text{T}}^{\text{miss}}$ variable is the magnitude of the negative vector sum of the transverse momenta, $-\sum_i \vec{p}_{\text{T},i}$, where i represents both the “hard objects” and the “soft term.” The hard objects consist of leptons and jets, which are individually reconstructed and calibrated; the list excludes pileup jets, which are removed by a jvt requirement. The soft term is formed from inner detector tracks not associated with the hard objects, but matched to the primary vertex. In the search region, the $E_{\text{T}}^{\text{miss}}$ produced by the Higgs decay is balanced in the transverse plane by the dijet system.

The jvt procedure is intended to remove pileup jets, but can cause large fake $E_{\text{T}}^{\text{miss}}$ if it removes a high- p_{T} jet from the hard scatter, e.g., a jet from a p_{T} -balanced three-jet event. In order to reduce this, a correlated quantity $H_{\text{T}}^{\text{miss}}$ —defined as $|\sum_j \vec{p}_{\text{T},j}|$, where j represents all jets without the jvt requirement—is required to be $H_{\text{T}}^{\text{miss}} > 150 \text{ GeV}$. In the three-jet example, $H_{\text{T}}^{\text{miss}}$ would be near zero.

The $E_{\text{T}}^{\text{miss}}$ significance (S_{MET}) is used only in events with one identified electron in the final state and is defined as $E_{\text{T}}^{\text{miss}} / \sqrt{p_{\text{T},j_1} + p_{\text{T},j_2} + p_{\text{T},e}}$, where the p_{T} quantities are for leading jet (j_1), subleading jet (j_2), and electron, respectively. The use of this quantity to reduce the contamination from jets misidentified as electrons is discussed in Section 5.

3. Event simulation

Monte Carlo simulation (MC) consists of an event generation followed by detector simulation [48] using GEANT4 [49]. Simulated events were corrected for the small differences between data and

³ The distance variable is defined as $\Delta R = \sqrt{(\Delta\eta)^2 + (\Delta\phi)^2}$.

MC in the trigger, the lepton identification efficiency, and the jet energy scale and resolution using dedicated data samples.

For the signal process, the VBF events were generated at next-to-leading order (NLO) in QCD using POWHEG-BOX2 [50]; inclusive NLO electroweak corrections were applied using HAWK [51]. The generated events were interfaced with PYTHIA8 [52] for hadronization and showering, using the AZNLO tune [53] and the NNPDF3.0 NNLO PDF set [54]. The gluon fusion events were generated using POWHEG-NNLOPS [55] with the PDF4LHC15 PDF set [56] interfaced to a fast detector simulation [57–59]. The cross section for ggF (VBF) was computed at N³LO (NNLO) in QCD and NLO (NLO) in electroweak. The showering simulation followed the same procedure as for the VBF sample. For both the VBF and gluon fusion events, the $H \rightarrow ZZ^* \rightarrow 4\nu$ process is included in the sample as invisible decays of the Higgs boson. Additional scalars with masses up to 3 TeV were simulated as described above for VBF signal process, assuming a full width of 4 MeV.

The W and Z events were generated using SHERPA2.2.1 [60] with COMIX [61] and OPENLOOPS [62] matrix-element generators, and merged with SHERPA parton shower [63] using the ME+PS@NLO prescription [64]. The NNPDF3.0 NNLO PDF set was used. In terms of the order of the various processes, the strong production was calculated at NLO for up to two jets and leading order (LO) for the third and fourth jets. The electroweak production was calculated at LO for the second and third jets. The levels of the interference between electroweak and strong processes were computed with MADGRAPH5_AMC@NLO [65]. The interference on the total expected background is only 0.1% and thus neglected.

Other potential background processes involve top quarks, dibosons, and multijets. Top quarks and dibosons were generated with POWHEG interfaced with PYTHIA and EVTGEN [66], which simulate the heavy-flavor decays. The diboson backgrounds include electroweak-mediated processes. The multijet estimate does not directly use the MC.

To each hard-scatter MC event, pileup collisions (30 on average) were added to mimic the environment of the LHC. The pileup collisions, simulated with PYTHIA8 [52] using MSTW2008 PDF [67] and the A2 set of tuned parameters [68], were subsequently reweighted to reproduce the pileup distribution in data.

The sizes of the MC samples vary depending on the process. The effective luminosity ranges for the MC samples varies depending on the process and on the selections, which are defined in Section 4. For the W process, the MC sample is approximately half of that of the data selected for the W control region and also half for the signal region. For the Z process, the MC sample for the $Z_{\ell\ell}$ subprocess is approximately twice that of data in the Z control region; the MC sample for $Z_{\nu\nu}$ subprocess is approximately the same as that of data in the signal region.

4. Event selection

All events must have a primary vertex. The selection listed below divides the data sample into a signal-enriched search region (SR) and background-enriched control regions (CR). The control regions and the statistical fit are discussed in detail in Section 5. The rest of this section focuses on the SR and the prefit event yields.⁴

For the SR, an event is required to have

- no isolated electron or muon,
- a leading jet with $p_T > 80$ GeV,
- a subleading jet with $p_T > 50$ GeV,

⁴ “Prefit” indicates that the event yields are not adjusted according to the statistical treatment of the background predictions, which is described in the second half of Section 5. “Postfit” labels the quantities that come out of the fit procedure.

Table 1

Event yields in the signal region (SR) and control regions (CR) summed over lepton charge and flavor. The yields are the *prefit* values for $m_{jj} > 1$ TeV. The observed data (N), the background estimate (B), and the signal (S for $m_H = 125$ GeV with $\mathcal{B}_{\text{inv}} = 1$) are given. The B and S values for individual processes are rounded to a precision commensurate with the sampling uncertainty associated with the finite MC sample size. For all processes the fractions of electroweak production [EW] are given. “Other” is defined in the text.

Description	SR		W CR		Z CR	
	Yield	[EW]	Yield	[EW]	Yield	[EW]
N , observed	2252		1602		166	
B , expected	2243		1648		183	
$Z \rightarrow \nu\nu$	1111	[18%]	–		–	
$Z \rightarrow ee, \mu\mu$	12	[9%]	38	[9%]	181	[23%]
$Z \rightarrow \tau\tau$	10	[16%]	11	[16%]	–	
$W \rightarrow e\nu, \mu\nu$	540	[16%]	1400	[30%]	–	
$W \rightarrow \tau\nu$	533	[20%]	130	[34%]	–	
Other	36		67		2	
S , signal	1070		–		–	
VBF	930		–		–	
Gluon fusion	140		–		–	

- no additional jets with $p_T > 25$ GeV,
- $E_T^{\text{miss}} > 180$ GeV,
- $H_T^{\text{miss}} > 150$ GeV.

The two jets are required to have the following properties:

- not be aligned with \vec{E}_T^{miss} , $|\Delta\phi_{j\text{-MET}}| > 1$,
- not be back-to-back, $|\Delta\phi_{jj}| < 1.8$,
- be well separated in η , $|\Delta\eta_{jj}| > 4.8$,
- be in opposite η hemispheres, $\eta_{j_1} \cdot \eta_{j_2} < 0$,
- $m_{jj} > 1$ TeV.

The SR includes background events containing a W or Z plus two jets, where the W decays into $e\nu$, $\mu\nu$, and $\tau\nu$, and the Z decays into two neutrinos. Here the leptons from the W decays are not reconstructed since they would otherwise be rejected by the selection.

Table 1 gives the prefit SR yields in the first column. The VBF production process gives the biggest contribution (87%) to the signal sample (fixed as $\mathcal{B}_{\text{inv}} = 1$). The contribution from gluon fusion accompanied by parton radiation is small (13%) and other production modes contribute negligibly. The fraction of VBF signal events that pass the signal region event selections, defined as acceptance times reconstruction efficiency, is 0.7%. As is discussed in Section 7, the signal significance is improved by considering three bins of m_{jj} defined as follows: $1 < m_{jj} \leq 1.5$ TeV, $1.5 < m_{jj} \leq 2$ TeV, and $m_{jj} > 2$ TeV. The prefit S/B ratio (for $\mathcal{B}_{\text{inv}} = 1$) in these bins is approximately 0.3, 0.4, 0.8, respectively.

For the backgrounds, both the strong production and the EW production contribute in the SR. The strong production processes contributes more than 70% of the backgrounds in all of the m_{jj} bins. There is variation in the EW fractions for the background processes due to a combination of the following factors: known differences in the production diagrams between W and Z , differences in kinematic acceptance for the particular W or Z decay, and differences in the MC sample size for each EW process.

5. Control samples and statistical treatment

The main backgrounds in the SR, comprising of 98% of the background, are the W and Z processes. The minor backgrounds, comprising the remaining 2%, are the diboson, $t\bar{t}$, and multijet processes. Accurate estimation of the W and Z processes is the biggest challenge of the analysis. The main background yields are extracted using dedicated control samples in data.

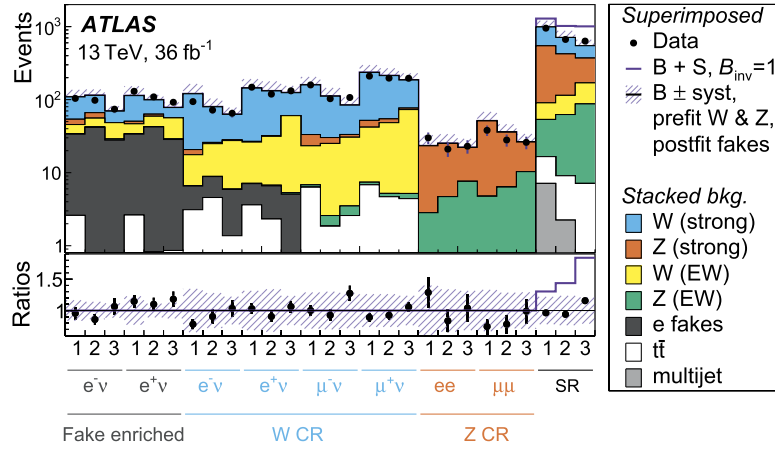


Fig. 1. Data-to-MC yield comparisons in the 27 subsamples used in the statistical fit. The observed data N (dots) are superimposed on the *prefit* backgrounds B (stacked histogram with shaded systematic uncertainty bands). The hypothetical signal S (empty blue histogram) is shown on top of B for $\mathcal{B}_{\text{inv}}=1$. The bottom panels show the ratios of N (dots) and $B+S$ (blue line) to B with the systematic uncertainty band shown on the line at 1. The 1, 2, and 3 bin labels corresponds to $1 < m_{jj} \leq 2 \text{ TeV}$, $1.5 < m_{jj} \leq 2 \text{ TeV}$, and $m_{jj} > 2 \text{ TeV}$, respectively. The “ e fakes” refers to $S_{\text{MET}} < 4 \sqrt{\text{GeV}}$ selection and is determined by the fit, so *postfit* values are shown for the purposes of illustration. The diboson contribution is included in the electroweak (EW) W and Z bosons.

This section is organized as follows. First, the two main CR are described and the associated *prefit* yields are given. Second, the fit parameters are defined along with a discussion of the contamination in the $W_{e\nu}$ subsample. Third, the fit procedure is described and the *postfit* yields are stated. Lastly, the minor backgrounds and the estimation of the multijet processes are described.

The W CR requires one identified lepton with a p_T threshold of 30 GeV , but the selections are otherwise identical to those of the SR. The initial $\ell\nu$ selection is divided by lepton flavor, charge, and, for the $e\nu$ final state, a passing selection on $S_{\text{MET}} > 4\sqrt{\text{GeV}}$ to define four W CR subsamples ($W_{\mu^+\nu}$, $W_{\mu^-\nu}$, $W_{e^+\nu}^{\text{HIGH}}$, $W_{e^-\nu}^{\text{HIGH}}$). The complementary failed selection on S_{MET} defines the two “fake-enriched” subsamples ($W_{e^+\nu}^{\text{LOW}}$, $W_{e^-\nu}^{\text{LOW}}$). The E_T^{miss} is calculated by adding the calibrated leptons to the sum.

The Z CR is based on the same selection criteria as the SR, but the lepton veto is replaced by the requirement of two same-flavor opposite-sign leptons ℓ with $|m_{\ell\ell} - m_Z| < 25 \text{ GeV}$. The sample is divided by lepton flavor, but not by charge (Z_{ee} , $Z_{\mu\mu}$). The leading lepton- p_T threshold is the same as above, and the subleading lepton- p_T threshold is 7 GeV . The E_T^{miss} is calculated as is done above.

Table 1 gives the *prefit* CR yields for the inclusive selection of $m_{jj} > 1 \text{ TeV}$ for the W (Z) CR in the third (fourth) columns. These *prefit* yields are the inputs for the statistical fit described below. The samples are very pure, as the relative contribution of the W (Z) CR is 95% (99%) from W (Z) decays. The definitions of the main normalizations parameters in the fit are

$$\begin{aligned} (B_W^{\text{SR}})_{\text{estimate}} &= N_W^{\text{CR}} \cdot B_W^{\text{SR}}/B_W^{\text{CR}} = B_W^{\text{SR}} \cdot N_W^{\text{CR}}/B_W^{\text{CR}} \\ (B_Z^{\text{SR}})_{\text{estimate}} &= N_Z^{\text{CR}} \cdot \underbrace{B_Z^{\text{SR}}/B_Z^{\text{CR}}}_{\alpha \text{ transfer}} = B_Z^{\text{SR}} \cdot \underbrace{N_Z^{\text{CR}}/B_Z^{\text{CR}}}_{\beta \text{ normalization}}, \end{aligned}$$

where the event yields are for the observed data (N) and the MC estimate of the background (B). The transfer factor α is the SR-to-CR ratio of the MC yields, and is a quantity useful for visualizing how the systematic uncertainties partially cancel out. The normalization β is the data-to-MC ratio in the CR, which is extracted from the fit. The analysis is performed in three m_{jj} bins i , so i also indexes α and β .

For the $W_{e\nu}^{\text{HIGH}}$ subsample in the W CR, a yield parameter ν_{fake} is introduced to quantify the “ e fakes,” the group of electron candidates that are not prompt electrons. This contamination occurs most often when a jet from a multijet event identified as an electron candidate. The underlying idea is that the W decays (multi-

jets) have high (low) E_T^{miss} resolution event-by-event. Since S_{MET} is a proxy for E_T^{miss} resolution, a passing (failing) selection on $S_{\text{MET}} > 4\sqrt{\text{GeV}}$ provides a $W_{e\nu}^{\text{HIGH}}$ ($W_{e\nu}^{\text{LOW}}$) subsample depleted (enriched) in e fakes. In the fake-enriched $W_{e\nu}^{\text{LOW}}$ subsample, about a third of the events are due to e fakes. (For the $W_{e\nu}$ process, the E_T^{miss} comes from the neutrino. For this reason, the kinematic bias in E_T^{miss} due to the S_{MET} selection was found to be negligible at the 1% level.) The resulting subsamples are tied together by a fixed ratio ρ_{fake} , which is determined using a separate “pure-fake” region.

The pure-fake region ($F_{e\nu}$) is defined by a selection on the electron likelihood (\mathcal{L}_e). Since \mathcal{L}_e is optimized to separate electrons from backgrounds originating from dijet processes [41], requiring that the candidate’s \mathcal{L}_e value fail the TIGHT definition [42], while satisfying a looser definition, selects the $F_{e\nu}$ data sample. As done above, the S_{MET} selection creates two subsamples ($F_{e\nu}^{\text{HIGH}}$, $F_{e\nu}^{\text{LOW}}$). The $F_{e\nu}^{\text{LOW}}$ -to- $F_{e\nu}^{\text{HIGH}}$ ratio of the number of events in data is ρ_{fake} , with the small amount of prompt W contamination subtracted using MC.

Model testing uses a profile likelihood-ratio test statistic [69] in the CL_s -modified frequentist formalism [70]. The statistical treatment considers a total of 27 bins: three m_{jj} bins for each of nine subsamples (one for the SR, four for the W CR, two for the fake-enriched subsamples, two for the Z CR). A maximum-likelihood fit to the observed data in each m_{jj} bin sets an upper limit,⁵ using a one-sided confidence level, on \mathcal{B}_{inv} for the 125 GeV Higgs boson and on the product $\sigma_{\text{scalar}}^{\text{VBF}} \cdot \mathcal{B}_{\text{inv}}$ for a scalar of different mass. The *prefit* comparisons of data and MC are shown for all subsamples in Fig. 1.

The fit procedure extracts the nine floating parameters introduced above (β_W , β_Z , ν_{fake} for each m_{jj} bin). After the fit, the *postfit* β parameters are consistent with the SM *prefit* prediction within their 1σ uncertainties. The *postfit* comparisons of data and expected backgrounds are shown in Fig. 2 for the two key variables, m_{jj} and E_T^{miss} , for the W and Z CR. The m_{jj} (E_T^{miss}) plot groups the backgrounds to show the dependence of the distribution shape on the production mechanism (final state).

⁵ The likelihood is a product of Poisson functions, one for each sample of N events while expecting λ , a Gaussian function for each systematic uncertainty, and a Poisson function for the number of MC events. In the simple scenario with only W and Z backgrounds, the λ for the SR would be $S + \beta_W \cdot B_W^{\text{SR}} + \beta_Z \cdot B_Z^{\text{SR}}$, with each quantity multiplied by the response function for a systematic uncertainty. For the W CR it is $\beta_W \cdot B_W^{\text{CR}}$ and for the Z CR it is $\beta_Z \cdot B_Z^{\text{CR}}$. See, e.g., Ref. [71].

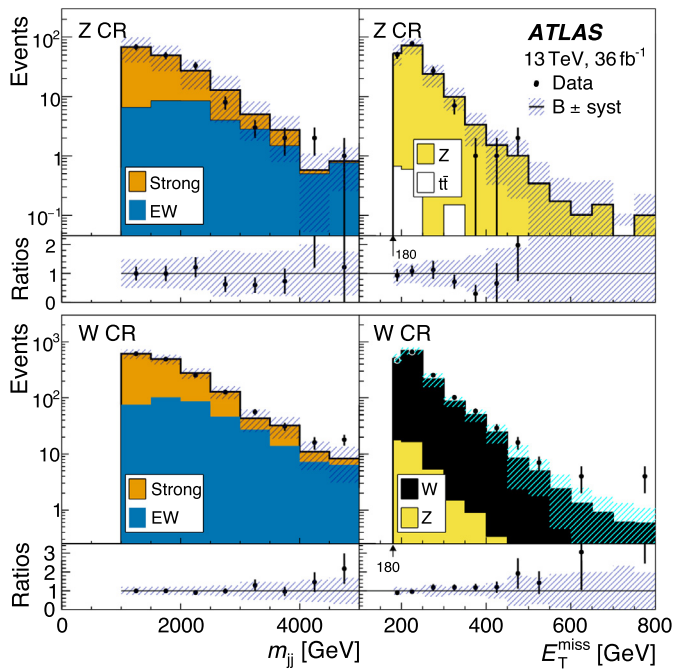


Fig. 2. Distribution of event yields in the Z (top) and W (bottom) control regions. The *postfit* normalizations for m_{jj} (left) and E_T^{miss} (right) are summed over the sub-samples. The E_T^{miss} distributions start at 180 GeV as indicated. The observed data N (dots) are superimposed on the sum of the backgrounds B (stacked histogram with shaded systematic uncertainty bands). The breakdown of the B is given in the lower left box in each panel. The bottom panels show the ratios of N to B with the systematic uncertainty band shown on the line at 1. The “other,” as listed in Table 1, contribute a few events at low values of m_{jj} and E_T^{miss} , and are omitted. The last bin in each plot contains the overflow.

The *postfit* value of ν_{fake} (the product $\rho_{\text{fake}} \cdot \nu_{\text{fake}}$) is the absolute number of e fake events in the $W_{\text{ev}}^{\text{HIGH}}$ ($W_{\text{ev}}^{\text{LOW}}$) subsamples. Since there is a ν_{fake} parameter for each bin i , the m_{jj} shape is also predicted. Apart from determining the ρ_{fake} value, which is fixed in the fit, F_{ev} is not part of the fit model. We note that the $W_{\text{ev}}^{\text{HIGH}} - W_{\text{ev}}^{\text{LOW}}$ samples are split by charge, because W^\pm production is not symmetric in pp collisions. However, the same ν_{fake} parameter is used for both charges because the e fakes are expected to be symmetric in charge since they originate mostly from multijet events.

The remaining processes—top quarks, dibosons, multijets—contribute negligibly to the SR (called “other” in Table 1). The first two are estimated with MC using nominal cross sections. The multijet contribution is very small, but it is a difficult process to estimate. It is a potentially dangerous background because those events that pass the E_T^{miss} selection are mostly due to instrumental effects.

The billionfold-or-more reduction of multijets after the event selection makes it impractical to simulate, so a data-driven method based on a rebalance-and-smear strategy [72] is used. The assumption is that the E_T^{miss} is due to jet mismeasurement in the detector response to jets and neutrinos from heavy-flavor decays [73,74]. Using the jet-triggered sample, the jet momenta are rebalanced by a kinematic fit, within their experimental uncertainties, to obtain the balanced value of the jets’ p_T . The rebalanced jets are smeared according to jet response templates, which are obtained from MC and validated with dijet data. The rebalance-and-smear method predicts both the shape of the E_T^{miss} distribution and the absolute normalization. The procedure is verified in a $\Delta\phi_{jj}$ -sideband validation region (VR) with 95% purity of QCD multijet events. This VR is defined by $1.8 < |\Delta\phi_{jj}| < 2.7$ and the loosening of the other requirements ($|\Delta\eta_{jj}| > 3$, $m_{jj} > 0.6\text{TeV}$, and allow a third leading jet with $25 < p_T < 50\text{GeV}$, but no other jets with $p_T > 25\text{GeV}$). The

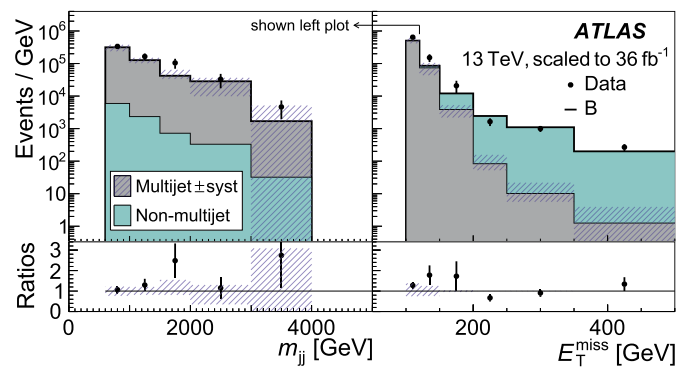


Fig. 3. Distribution of event yields in the multijet validation region for m_{jj} (left) and E_T^{miss} (right). The m_{jj} plot shows the $100 < E_T^{\text{miss}} < 120\text{GeV}$ subset of the right plot as indicated by the arrow. The N observed data (dots) are superimposed on the sum of the B backgrounds (stacked histogram). The systematic uncertainty band applies only to the multijet component. The statistical uncertainties are relatively large because of the weighting of the trigger samples with large prescale values. See the caption of Fig. 2 for other plotting details.

comparison of the predictions and the data in the VR shows good agreement (Fig. 3). The multijet component is obtained using the rebalance-and-smear method with the associated systematic uncertainty bands, while the non-multijet components are obtained using MC.

6. Uncertainties

Experimental and theoretical sources of uncertainties as well as the correlations between the various sources are described. The resulting impact of the uncertainties on the yields and on the signal sensitivity is summarized later in Table 2.

Experimental sources of uncertainty are due mainly to the jet energy scale and resolution [75], E_T^{miss} soft term [76], and lepton measurements [42,43]. In order to reduce fluctuations due to limited MC sample size, the uncertainties in number of expected events for the variations of jet energy scale and resolution for the strong and electroweak background samples are averaged. This is motivated by the similarities of the kinematics and the detector effects for the two production processes for each m_{jj} bin. The uncertainty related to lepton identification or veto has a non-negligible (negligible) effect on α_W (α_Z) because of the following scenarios. The W_{ev} background is significant in the SR, which results in an uncertainty for the cases related to the lepton veto. The $Z_{\ell\ell}$ background is negligible in the SR, because the selection requires there to be no leptons.

The following experimental sources have small or negligible impact in the final result. The pileup distribution and luminosity [77,78] have a relatively small impact. The trigger efficiency modeling, for both the lepton triggers for the CR and E_T^{miss} triggers for the SR, are not listed in Table 2. Their impact on the events yields was at the 1% level and their impact on the signal sensitivity are found to be negligible.

Theoretical sources of uncertainty are due mainly to scale choices in fixed-order matrix-element calculations. For the background processes, QCD scales are varied for the resummation scale (resum.), renormalization scale (renorm.), factorization scale (fact.), and cKw matching scale. The first three scales in the list—technically called q^2 , μ_R , μ_F , respectively—are varied by a factor of two [79,80]. For the cKw matching scale between the matrix element and the parton shower [60], the central value and the considered variations are 20_{-5}^{+10}GeV . The higher-order electroweak corrections to the strongly produced W or Z are found to be negligible.

Table 2
Sources of uncertainty. The first set shows Δ , the relative improvement of the 95% CL upper limit on \mathcal{B}_{inv} when the source of uncertainty is “removed” by fixing it to its best-fit value. The “visual” column shows bars whose lengths from the center tick are proportional to Δ . The second set shows the effect on the yields and the α transfer factors for the $1 < m_{jj} \leq 1.5$ TeV bin. The yields are for the signal process in the SR (S), Z MC in the SR (B_{SR}^Z), and Z MC in the CR (B_{CR}^Z). The α_Z is given to demonstrate the reduction in the uncertainty in the ratio $B_{\text{SR}}^Z/B_{\text{CR}}^Z$. The individual yields for the W are not shown because the cancellation effects are similar to the Z counterparts. The value for “3rd jet veto” corresponds only to the uncertainty related to jet bin migration for signal processes; the corresponding effect for the background processes are evaluated in the various jet energy and theoretical variations. The abbreviations for the theoretical sources are described in the text. The ‘-’ indicates that the quantity is not applicable. The “combined” rows at the bottom are not simple sums of the rows above because of the Δ metric; the symbols (\dagger, \ddagger, \star) are parenthetically defined in the table. The penultimate (last) row shows the summary impact of removing the systematic uncertainties due to the experimental and theoretical sources (as well as statistical uncertainties of the MC samples).

Source	\mathcal{B}_{inv} improve. [%] using all m_{jj} bins		Yields, α changes (%) in $1 < m_{jj} \leq 1.5$ TeV				
	Δ	visual	S	B_{SR}^Z	B_{CR}^Z	α_Z	α_W
Experimental (\dagger)							
Jet energy scale	10		12	7	8	8	6
Jet energy resol.	2		2	0	1	1	4
$E_{\text{T}}^{\text{miss}}$ soft term	1		2	2	2	2	2
Lepton id., veto	2		-	-	-	0	4
Pileup distrib.	1		3	1	2	3	1
Luminosity	0		2	2	2	-	-
Theoretical (\ddagger)							
Resum. scale	1		-	2	3	0	2
Renorm., fact.	2		-	20	19	1	2
ckkw matching	4		-	2	3	1	5
PDF	0		1	1	2	1	1
3rd jet veto	2		7	-	-	-	-
Statistical							
MC sample (\star)	12		4	5	9	10	9
Data sample	21		6	5	12	12	6
Combined							
All \dagger sources	17						
All \ddagger sources	10						
Combine \dagger, \ddagger	28						
Combine \dagger, \ddagger, \star	42						

The effects of the theoretical variations are evaluated with a sample of generated MC events prior to reconstruction, which is larger than the reconstructed sample. Moreover, in order to reduce fluctuations due to limited MC statistics, the effect of the resummation and ckkw variations as a function of m_{jj} are determined by a linear fit, using m_{jj} values below the selection for the SR and a sample with loosened selection on $\Delta\eta_{jj}$ and $\Delta\phi_{jj}$. We verified that an additional systematic uncertainty associated with the extrapolation is dominated by the statistical fluctuations in the varied samples.

For both signal and background, the effects of the choice of a parton distribution function (PDF) set have a relatively small impact. The variations are considered using an ensemble of PDFs within the NNPDF set [54] and the standard deviation of the distribution is taken as the uncertainty.

For the signal process, the effect of the scale uncertainty on the third-jet veto for the gluon fusion plus two-jet contribution is evaluated using the jet-bin method [81]. The similar effect for the VBF contribution is evaluated by comparing the scale varied samples before and after the third-jet veto. The impact on the Higgs signal yield is dominated by the VBF contribution, which is around 7%.

Statistical uncertainties are due to the data and MC sample sizes.

Systematic uncertainties are assumed to be either fully correlated or uncorrelated. The uncertainties from the following sources in each independent m_{jj} bin are correlated between the SR and CR: QCD scales, PDF, and lepton measurements. The theoretical uncertainties due to QCD scales are uncorrelated between the following pairs: signal vs. background, electroweak vs. strong production, and W vs. Z production. Theoretical uncertainties are fully uncorrelated between bins of m_{jj} , while the experimental uncertainties are fully correlated, both of which are expected to be conservative assumptions.

One major difference between Ref. [28] and this paper—with the former (latter) employing (not employing) the W -to- Z extrapolation strategy—is that we now have a larger $Z_{\ell\ell}$ control sample. We found that the final limit result based on the statistical uncertainty of the enlarged $Z_{\ell\ell}$ control sample is similar to the result assuming the theoretical uncertainties on the W -to- Z ratio (including the associated MC sample statistical uncertainties). This being the case, this paper adopts the method that is less dependent on theoretical assumptions.

The sources of uncertainty are grouped into the three main categories given above (Table 2). The impact of each source is measured in two ways: (1) on the 95% CL upper limit on \mathcal{B}_{inv} and (2) on the event yields and α transfer factors. Impact (1) assesses the percentage improvement of the \mathcal{B}_{inv} limit if that source of uncertainty is removed after fixing the associated parameter to its best-fit value. Impact (2) demonstrates that the systematic uncertainties in the individual yields partially cancel out for many of the theoretical sources. However, for many of the experimental sources the cancellation is not achieved due to limited MC statistics of the varied samples. For example, the effects of varying the renormalization and factorization scales change the MC yield in the Z SR (B_{SR}^Z in Table 2) and the Z CR (B_{CR}^Z) by about 20%, but the α_Z transfer factor changes by only 1%. In Table 2, only the $1 < m_{jj} \leq 1.5$ TeV yields are shown for the purpose of illustrating the partial cancellation in the ratio.

In general, the uncertainties are higher with m_{jj} . The MC sample statistics is the largest source of systematic uncertainties, with the uncertainty increasing with m_{jj} due to limited number of simulated events. The theory uncertainties are also higher with m_{jj} values for the same reason. The experimental jet energy uncertainties are also affected by the limited sample size, with larger fluctuations because of fluctuations that do not cancel for each individual systematic variations. For the sources contributing the

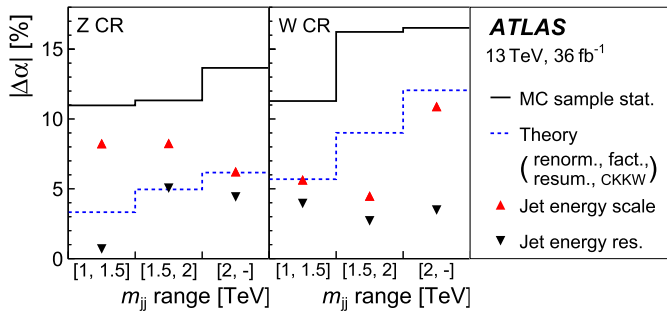


Fig. 4. Contributions to the relative uncertainty in the transfer factors α_Z (left) and α_W (right) in the three m_{jj} bins of the SR. The theoretical uncertainties from the sources noted in the legend are combined in quadrature.

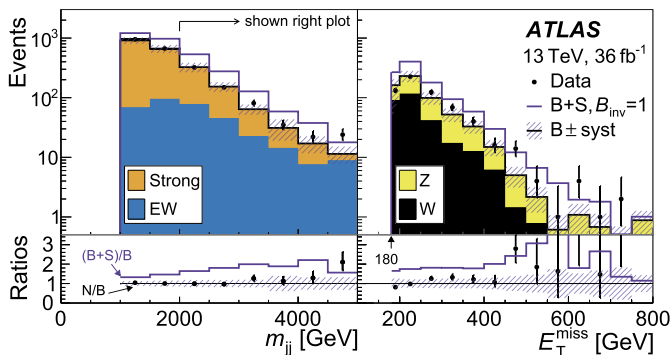


Fig. 5. Distribution of event yields in the signal region for m_{jj} (left) and E_T^{miss} (right). The E_T^{miss} distributions start at 180 GeV and shows the most sensitive $m_{jj} > 2$ TeV subset of the SR as indicated by the arrow. The *postfit* normalizations for m_{jj} (E_T^{miss}) distributions use separate background, B , normalizations in the three (one) m_{jj} bins of $1 < m_{jj} \leq 1.5$ TeV, $1.5 < m_{jj} \leq 2$ TeV, and $m_{jj} > 2$ TeV ($m_{jj} > 2$ TeV), and sum the contributions from W and Z bosons (electroweak and strong production modes). The hypothetical signal S (empty blue histogram) is shown on top of B for $\mathcal{B}_{\text{inv}} = 1$. The bottom panels show the ratios of N (dots) and $B+S$ (blue line) to B with the systematic uncertainty band shown on the line at 1. The bin width in the m_{jj} plots (E_T^{miss}) is 500 GeV (50 GeV except for the first bin with the non-zero entry, which is 20 GeV). See the caption of Fig. 2 for other plotting details.

largest uncertainties, the α_Z and the α_W variations in the three m_{jj} bins are shown graphically in Fig. 4.

The combination of uncertainties from various sources shows that the dominant category has a systematic origin (penultimate row of Table 2). The lack of MC statistical precision for background processes with $m_{jj} > 2$ TeV has the largest impact on \mathcal{B}_{inv} . We note that the Δ values are percent improvements of the final limit on \mathcal{B}_{inv} , so they do not add in quadrature or in any such standard statistical combinations.

7. Results and interpretations

The 2252 observed events in the SR are divided among the three m_{jj} bins defined previously: 952, 667, and 633 events. These values are consistent with the background-only *postfit* yields of the sum of the background processes of 2100 events, which are divided among the three m_{jj} bins: 850 ± 113 , 660 ± 90 , and 590 ± 81 , respectively. The uncertainty represents the combined effect due to experimental and theoretical systematic uncertainties. These *postfit* values are also consistent with the *prefit* predictions. The expected signal yields (for $\mathcal{B}_{\text{inv}} = 1$ for VBF and gluon fusion) are 300, 310, and 460, respectively, and the last m_{jj} bin has the highest sensitivity with $S/B \approx 0.8$.

The *postfit* SR event distributions of m_{jj} and E_T^{miss} are shown in Fig. 5, and we observe agreement, within uncertainties, between the data and the expected backgrounds.

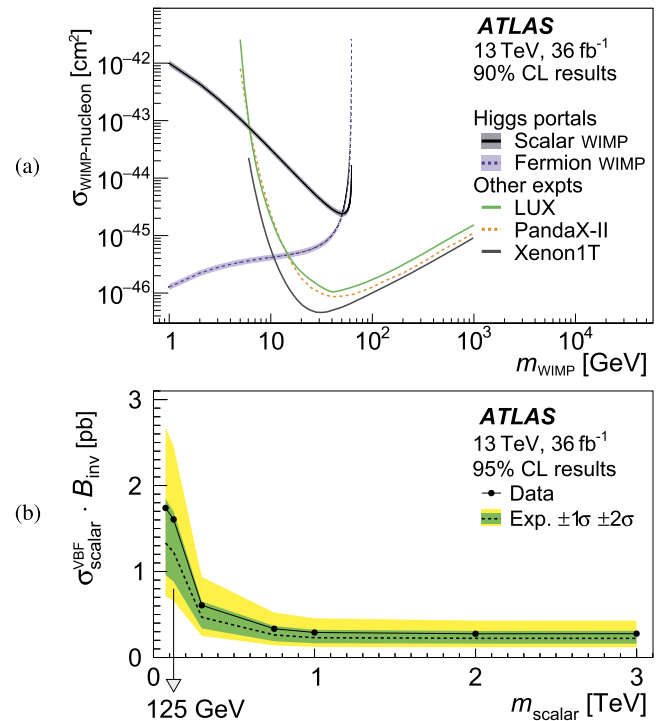


Fig. 6. Upper limits on (a) the spin-independent WIMP–nucleon cross section using Higgs portal interpretations of \mathcal{B}_{inv} at 90% CL vs. m_{WIMP} and (b) the VBF cross section times the branching fraction to invisible decays at 95% CL vs. m_{scalar} . The top plot shows results from Ref. [85–87].

The left plot in Fig. 5 also shows that the S/B ratio rises with increasing m_{jj} values, which motivates our division of the SR into multiple bins. The total electroweak contribution in the SR is relatively small at $\mathcal{O}(10\%)$ (Table 1), but the much flatter distribution of m_{jj} makes it an important contribution to the final result. As noted in Section 5, the background estimation is done independently for each m_{jj} bin to reduce the dependence on m_{jj} modeling.

The fit, assuming the 125 GeV Higgs boson, gives the observed (expected) upper limit on \mathcal{B}_{inv} of 0.37 ($0.28^{+0.11}_{-0.08}$) at 95% CL, and 0.32 ($0.23^{+0.11}_{-0.10}$) at 90% CL, where the uncertainties placed on the expected limit represent the 1σ variations. With this result, connections to WIMP dark matter can be made in the context of Higgs portal models [82]. The limit on \mathcal{B}_{inv} can be used to set limit on the Higgs-wimp coupling by the WIMP-nucleon scattering cross section formulae ($\sigma_{\text{WIMP-nucleon}}$). In this paper, scalar and Majorana fermion WIMP models are considered [11,83,84].

The overlay of the interpretation of this result with the limits from some of the direct detection experiments [85–87] shows the complementarity in coverage (Fig. 6(a)). For the scalar WIMP interpretation cross sections are excluded at values ranging from $\mathcal{O}(10^{-42})$ to $\mathcal{O}(10^{-45})$ cm^2 and for the Majorana fermion WIMP interpretation the exclusion range is from $\mathcal{O}(10^{-45})$ to $\mathcal{O}(10^{-46})$ cm^2 , depending on the WIMP mass. The uncertainty band in the plot uses an updated computation of the nucleon form factors [88].

The correlation between \mathcal{B}_{inv} and $\sigma_{\text{WIMP-nucleon}}$ is presented in the effective field theory framework assuming that the new-physics scale is $\mathcal{O}(1)$ TeV [28], well above the scale probed at the Higgs boson mass. Adding a renormalizable mechanism for generating the fermion WIMP masses could modify the above-mentioned correlation [89].

In place of the 125 GeV Higgs boson, the same selection is applied to additional scalars with masses (m_{scalar}) of up to 3 TeV assuming only VBF production. The fraction of VBF signal events that pass the signal region event selections corresponding to the

acceptance times efficiency ranges from 0.6–3%. The signal efficiency for the inclusive $m_{jj} > 1\text{ TeV}$ selection increases with the mass of the scalar boson, because the VBF jets is more forward with higher mass, and thus have more events at higher values of m_{jj} . The limit on $\sigma_{\text{scalar}}^{\text{VBF}} \cdot \mathcal{B}_{\text{inv}}$ as a function of m_{scalar} is shown in Fig. 6(b). The 95% confidence level upper limits on the cross section times branching fraction are in the range of 0.3–1.7 pb.

8. Conclusions

A search for Higgs boson decays into invisible particles is presented using the 36.1 fb^{-1} of pp collision data taken at $\sqrt{s} = 13\text{ TeV}$ collected in 2015 and 2016 by the ATLAS detector at the LHC. The targeted signature is the VBF topology with two energetic jets with a wide gap in η and large $E_{\text{T}}^{\text{miss}}$.

Assuming the Standard Model cross section for the 125 GeV Higgs boson, an upper limit of 0.37 is set on \mathcal{B}_{inv} at 95% CL. This result is interpreted using Higgs portal models to exclude regions in the $\sigma_{\text{WIMP-nucleon}}$ vs. m_{WIMP} parameter space to exclude cross section values ranging from $\mathcal{O}(10^{-42})$ to $\mathcal{O}(10^{-46})\text{ cm}^2$, depending on the WIMP mass and the WIMP model.

Searches for invisible decays of scalars with masses of up to 3 TeV are reported for the first time from ATLAS in the VBF production mode. These results are rather general and can be used for further interpretations.

Acknowledgements

We thank CERN for the very successful operation of the LHC, as well as the support staff from our institutions without whom ATLAS could not be operated efficiently.

We acknowledge the support of ANPCyT, Argentina; YerPhI, Armenia; ARC, Australia; BMWFW and FWF, Austria; ANAS, Azerbaijan; SSTC, Belarus; CNPq and FAPESP, Brazil; NSERC, NRC and CFI, Canada; CERN; CONICYT, Chile; CAS, MOST and NSFC, China; COLCIENCIAS, Colombia; MSMT CR, MPO CR and VSC CR, Czech Republic; DNRF and DNSRC, Denmark; IN2P3-CNRS, CEA-DRF/IRFU, France; SRNSFG, Georgia; BMBF, HGF, and MPG, Germany; GSRT, Greece; RGC, Hong Kong SAR, China; ISF and Benozziyo Center, Israel; INFN, Italy; MEXT and JSPS, Japan; CNRST, Morocco; NWO, Netherlands; RCN, Norway; MNISW and NCN, Poland; FCT, Portugal; MNE/IFA, Romania; MES of Russia and NRC KI, Russian Federation; JINR; MESTD, Serbia; MSSR, Slovakia; ARRS and MIZŠ, Slovenia; DST/NRF, South Africa; MINECO, Spain; SRC and Wallenberg Foundation, Sweden; SERI, SNSF and Cantons of Bern and Geneva, Switzerland; MOST, Taiwan; TAEK, Turkey; STFC, United Kingdom; DOE and NSF, United States of America. In addition, individual groups and members have received support from BCKDF, Canarie, CRC and Compute Canada, Canada; COST, ERC, ERDF, Horizon 2020, and Marie Skłodowska-Curie Actions, European Union; Investissements d' Avenir Labex and IDEX, ANR, France; DFG and AvH Foundation, Germany; Herakleitos, Thales and Aristeia programmes co-financed by EU-ESF and the Greek NSRF, Greece; BSF-NSF and GIF, Israel; CERCA Programme Generalitat de Catalunya, Spain; The Royal Society and Leverhulme Trust, United Kingdom.

The crucial computing support from all WLCG partners is acknowledged gratefully, in particular from CERN, the ATLAS Tier-1 facilities at TRIUMF (Canada), NDGF (Denmark, Norway, Sweden), CC-IN2P3 (France), KIT/GridKA (Germany), INFN-CNAF (Italy), NL-T1 (Netherlands), PIC (Spain), ASGC (Taiwan), RAL (UK) and BNL (USA), the Tier-2 facilities worldwide and large non-WLCG resource providers. Major contributors of computing resources are listed in Ref. [90].

References

- [1] ATLAS Collaboration, Observation of a new particle in the search for the Standard Model Higgs boson with the ATLAS detector at the LHC, Phys. Lett. B 716 (2012) 1, arXiv:1207.7214 [hep-ex].
- [2] CMS Collaboration, Observation of a new boson at a mass of 125 GeV with the CMS experiment at the LHC, Phys. Lett. B 716 (2012) 30, arXiv:1207.7235 [hep-ex].
- [3] S. Dittmaier, C. Mariotti, G. Passarino, R. Tanaka (Eds.), Handbook of LHC Higgs Cross Sections: 1. Inclusive Observables, 2011, CERN-2011-002, arXiv:1101.0593 [hep-ph].
- [4] S. Dittmaier, C. Mariotti, G. Passarino, R. Tanaka (Eds.), Handbook of LHC Higgs Cross Sections: 2. Differential Distributions, 2012, CERN-2012-002, arXiv:1201.3084 [hep-ph].
- [5] I. Antoniadis, M. Tuckmantel, F. Zwirner, Phenomenology of a leptonic goldstino and invisible Higgs boson decays, Nucl. Phys. B 707 (2005) 215, arXiv:hep-ph/0410165.
- [6] N. Arkani-Hamed, S. Dimopoulos, G.R. Dvali, J. March-Russell, Neutrino masses from large extra dimensions, Phys. Rev. D 65 (2002) 024032, arXiv:hep-ph/9811448.
- [7] S. Kanemura, S. Matsumoto, T. Nabeshima, N. Okada, Can WIMP dark matter overcome the nightmare scenario?, Phys. Rev. D 82 (2010) 055026, arXiv:1005.5651 [hep-ph].
- [8] A. Djouadi, O. Lebedev, Y. Mambrini, J. Quevillon, Implications of LHC searches for Higgs-portal dark matter, Phys. Lett. B 709 (2012) 65, arXiv:1112.3299 [hep-ph].
- [9] R.E. Shrock, M. Suzuki, Invisible decays of Higgs bosons, Phys. Lett. B 110 (1982) 250.
- [10] D. Choudhury, D.P. Roy, Signatures of an invisibly decaying Higgs particle at LHC, Phys. Lett. B 322 (1994) 368, arXiv:hep-ph/9312347.
- [11] O.J.P. Eboli, D. Zeppenfeld, Observing an invisible Higgs boson, Phys. Lett. B 495 (2000) 147, arXiv:hep-ph/0009158.
- [12] H. Davoudiasl, T. Han, H.E. Logan, Discovering an invisibly decaying Higgs at hadron colliders, Phys. Rev. D 71 (2005) 115007, arXiv:hep-ph/0412269.
- [13] R.M. Godbole, M. Guchait, K. Mazumdar, S. Moretti, D.P. Roy, Search for 'invisible' Higgs signals at LHC via associated production with gauge bosons, Phys. Lett. B 571 (2003) 184, arXiv:hep-ph/0304137.
- [14] D. Ghosh, R. Godbole, M. Guchait, K. Mohan, D. Sengupta, Looking for an invisible Higgs signal at the LHC, Phys. Lett. B 725 (2013) 344, arXiv:1211.7015 [hep-ph].
- [15] G. Belanger, B. Dumont, U. Ellwanger, J.F. Gunion, S. Kraml, Status of invisible Higgs decays, Phys. Lett. B 723 (2013) 340, arXiv:1302.5694 [hep-ph].
- [16] D. Curtin, R. Essig, S. Gori, P. Jaiswal, A. Katz, Tao Liu, Zhen Liu, D. McKeen, J. Shelton, M. Strassler, Z. Surujon, B. Tweedie, Y.-M. Zhong, Exotic decays of the 125 GeV Higgs boson, Phys. Rev. D 90 (2014) 075004, arXiv:1312.4992 [hep-ph].
- [17] H. Goldberg, Constraint on the photino mass from cosmology, Phys. Rev. Lett. 50 (1983) 1419.
- [18] J.R. Ellis, J.S. Hagelin, D.V. Nanopoulos, K.A. Olive, M. Srednicki, Supersymmetric relics from the big bang, Nucl. Phys. B 238 (1984) 453.
- [19] D. Clowe, et al., A direct empirical proof of the existence of dark matter, Astrophys. J. 648 (2006) L109, arXiv:astro-ph/0608407.
- [20] D. de Florian, C. Grojean, F. Maltoni, C. Mariotti, A. Nikitenko, M. Pieri, P. Savard, M. Schumacher, R. Tanaka (Eds.), Handbook of LHC Higgs Cross Sections: 4. Deciphering the Nature of the Higgs Sector, FERMILAB-FN-1025-T, 2016, CERN-2017-002-M, arXiv:1610.07922 [hep-ph], 2016.
- [21] ATLAS Collaboration, Search for invisible particles produced in association with single-top-quarks in proton-proton collisions at $\sqrt{s} = 8\text{ TeV}$ with the ATLAS detector, Eur. Phys. J. C 75 (2015) 79, arXiv:1410.5404 [hep-ex].
- [22] CMS Collaboration, Search for invisible decays of Higgs bosons in the vector boson fusion and associated ZH production modes, Eur. Phys. J. C 74 (2014) 2980, arXiv:1404.1344 [hep-ex].
- [23] ATLAS Collaboration, Search for invisible decays of the Higgs boson produced in association with a hadronically decaying vector boson in pp collisions at $\sqrt{s} = 8\text{ TeV}$ with the ATLAS detector, Eur. Phys. J. C 75 (2015) 337, arXiv:1504.04324 [hep-ex].
- [24] CMS Collaboration, Search for dark matter in proton-proton collisions at 8 TeV with missing transverse momentum and vector boson tagged jets, J. High Energy Phys. 12 (2016) 083, Erratum: J. High Energy Phys. 08 (2017) 035, arXiv:1607.05764 [hep-ex].
- [25] ATLAS Collaboration, Search for an invisibly decaying Higgs boson or dark matter candidates produced in association with a Z boson in pp collisions at $\sqrt{s} = 13\text{ TeV}$ with the ATLAS detector, Phys. Lett. B 776 (2018) 318, arXiv:1708.09624 [hep-ex].
- [26] ATLAS Collaboration, Combination of searches for invisible Higgs boson decays with the ATLAS experiment, <http://cds.cern.ch/record/2649407>, 2018.
- [27] CMS Collaboration, Search for invisible decays of a Higgs boson produced through vector boson fusion in proton-proton collisions at $\sqrt{s} = 13\text{ TeV}$, arXiv:1809.05937 [hep-ex], 2018.

- [28] ATLAS Collaboration, Search for invisible decays of a Higgs boson using vector-boson fusion in pp collisions at $\sqrt{s} = 8$ TeV with the ATLAS detector, *J. High Energy Phys.* 01 (2016) 172, arXiv:1508.07869 [hep-ex].
- [29] CMS Collaboration, Searches for invisible decays of the Higgs boson in pp collisions at $\sqrt{s} = 7, 8,$ and 13 TeV, *J. High Energy Phys.* 02 (2017) 135, arXiv:1610.09218 [hep-ex].
- [30] ATLAS Collaboration, Constraints on new phenomena via Higgs boson couplings and invisible decays with the ATLAS detector, *J. High Energy Phys.* 11 (2015) 206, arXiv:1509.00672 [hep-ex].
- [31] CMS Collaboration, Precise determination of the mass of the Higgs boson and tests of compatibility of its couplings with the standard model predictions using proton collisions at 7 and 8 TeV, *Eur. Phys. J. C* 75 (2015) 212, arXiv:1412.8662 [hep-ex].
- [32] ATLAS and CMS Collaborations, Measurements of the Higgs boson production and decay rates and constraints on its couplings from a combined ATLAS and CMS analysis of the LHC pp collision data at $\sqrt{s} = 7$ and 8 TeV, *J. High Energy Phys.* 08 (2016) 045, arXiv:1606.02266 [hep-ex].
- [33] CMS Collaboration, Combined measurements of Higgs boson couplings in proton-proton collisions at $\sqrt{s} = 13$ TeV, arXiv:1809.10733 [hep-ex], 2018.
- [34] ATLAS Collaboration, The ATLAS experiment at the CERN Large Hadron Collider, *J. Instrum.* 3 (2008) S08003.
- [35] ATLAS Collaboration, The ATLAS transverse-momentum trigger performance at the LHC in 2011, ATLAS-CONF-2014-002, <http://cds.cern.ch/record/1647616>, 2014.
- [36] ATLAS Collaboration, Analytical description of missing transverse-momentum trigger rates in ATLAS with 7 and 8 TeV data, ATL-DAQ-PUB-2017-002, <http://cds.cern.ch/record/2292378>, 2017.
- [37] ATLAS TDAQ Collaboration, The ATLAS data acquisition and high level trigger system, *J. Instrum.* 11 (2016) P06008.
- [38] ATLAS Collaboration, Topological cell clustering in the ATLAS calorimeters and its performance in LHC Run 1, *Eur. Phys. J. C* 77 (2017) 490, arXiv:1603.02934 [hep-ex].
- [39] ATLAS Collaboration, Performance of the ATLAS trigger system in 2015, *Eur. Phys. J. C* 77 (2017) 317, arXiv:1611.09661 [hep-ex].
- [40] ATLAS Collaboration, Trigger menu in 2016, ATL-DAQ-PUB-2017-001, <http://cds.cern.ch/record/2242069>, 2017.
- [41] ATLAS Collaboration, Electron efficiency measurements with the ATLAS detector using 2012 LHC proton-proton collision data, *Eur. Phys. J. C* 77 (2017) 195, arXiv:1612.01456 [hep-ex].
- [42] ATLAS Collaboration, Electron efficiency measurements with the ATLAS detector using the 2015 LHC proton-proton collision data, ATLAS-CONF-2016-024, <http://cds.cern.ch/record/2157687>, 2016.
- [43] ATLAS Collaboration, Muon reconstruction performance of the ATLAS detector in proton-proton collision data at $\sqrt{s} = 13$ TeV, *Eur. Phys. J. C* 76 (2016) 292, arXiv:1603.05598 [hep-ex].
- [44] M. Cacciari, G.P. Salam, G. Soyez, Anti- k_r jet clustering algorithm, *J. High Energy Phys.* 04 (2008) 063, arXiv:0802.1189 [hep-ex].
- [45] ATLAS Collaboration, Performance of pile-up mitigation techniques for jets in pp collisions at $\sqrt{s} = 8$ TeV using the ATLAS detector, *Eur. Phys. J. C* 76 (2016) 581, arXiv:1510.03823 [hep-ex].
- [46] ATLAS Collaboration, Selection of jets produced in 13 TeV proton-proton collisions with the ATLAS detector, ATLAS-CONF-2015-029, <http://cds.cern.ch/record/2037702>, 2015.
- [47] ATLAS Collaboration, Search for squarks and gluinos in final states with hadronically decaying τ -leptons, jets, and missing transverse momentum using pp collisions at $\sqrt{s} = 13$ TeV with the ATLAS detector, *Phys. Rev. D* 99 (2019) 012009, arXiv:1808.06358 [hep-ex].
- [48] ATLAS Collaboration, The ATLAS simulation infrastructure, *Eur. Phys. J. C* 70 (2010) 823, arXiv:1005.4568 [physics.ins-det].
- [49] GEANT4 Collaboration, GEANT4—a simulation toolkit, *Nucl. Instrum. Methods A* 506 (2003) 250.
- [50] P. Nason, C. Oleari, NLO Higgs boson production via vector-boson fusion matched with shower in POWHEG [POWHEG-BOX r1655], *J. High Energy Phys.* 02 (2010) 037, arXiv:0911.5299 [hep-ph].
- [51] M. Ciccolini, A. Denner, S. Dittmaier, Electroweak and QCD corrections to Higgs production via vector-boson fusion at the LHC, *Phys. Rev. D* 77 (2003) 013002, arXiv:0710.4749 [hep-ex].
- [52] T. Sjöstrand, S. Mrenna, P.Z. Skands, A brief introduction to PYTHIA 8.1, *Comput. Phys. Commun.* 178 (2008) 852, arXiv:0710.3820 [hep-ph].
- [53] ATLAS Collaboration, Measurement of the Z/γ^* boson transverse momentum distribution in pp collisions at $\sqrt{s} = 7$ TeV with the ATLAS detector, *J. High Energy Phys.* 09 (2014) 145, arXiv:1406.3660 [hep-ex].
- [54] R.D. Ball, et al., Parton distributions for the LHC Run II, *J. High Energy Phys.* 04 (2015) 040, arXiv:1410.8849 [hep-ph].
- [55] K. Hamilton, P. Nason, E. Re, G. Zanderighi, NNLOPS simulation of Higgs boson production, *J. High Energy Phys.* 10 (2013) 222, arXiv:1309.0017 [hep-ph].
- [56] J. Butterworth, et al., PDF4LHC recommendations for LHC Run II, *J. Phys. G* 43 (2016) 023001, arXiv:1510.03865 [hep-ph].
- [57] W. Lukas, Fast simulation for ATLAS: Atfast-II and ISF, *J. Phys. Conf. Ser.* 396 (2012) 022031.
- [58] ATLAS Collaboration, E_T^{miss} performance in the ATLAS detector using 2015–2016 LHC pp collisions, ATLAS-CONF-2018-023, <http://cds.cern.ch/record/2625233>, 2018.
- [59] ATLAS Collaboration, FastCaloSim performance plots, SIM-2018-001, <http://cern.ch/Atlas/GROUPS/PHYSICS/PLOTS/SIM-2018-001/>, 2018.
- [60] T. Gleisberg, et al., Event generation with SHERPA 1.1, *J. High Energy Phys.* 02 (2009) 007, arXiv:0811.4622 [hep-ph].
- [61] T. Gleisberg, S. Hoeche, Comix, a new matrix element generator, *J. High Energy Phys.* 12 (2008) 039, arXiv:0808.3674 [hep-ph].
- [62] F. Cascioli, P. Maierhofer, S. Pozzorini, Scattering amplitudes with open loops, *Phys. Rev. Lett.* 108 (2012) 111601, arXiv:1111.5206 [hep-ph].
- [63] S. Schumann, F. Krauss, A parton shower algorithm based on Catani-Seymour dipole factorisation, *J. High Energy Phys.* 03 (2008) 038, arXiv:0709.1027 [hep-ph].
- [64] S. Hoeche, F. Krauss, M. Schonherr, F. Siegert, QCD matrix elements + parton showers. The NLO case, *J. High Energy Phys.* 04 (2013) 027, arXiv:1207.5030 [hep-ph].
- [65] J. Alwall, et al., The automated computation of tree-level and next-to-leading order differential cross sections, and their matching to parton shower simulations, *J. High Energy Phys.* 07 (2014) 079, arXiv:1405.0301 [hep-ph].
- [66] D.J. Lange, The EvtGen particle decay simulation package, *Nucl. Instrum. Methods A* 462 (2001) 152.
- [67] A.D. Martin, W.J. Stirling, R.S. Thorne, G. Watt, Parton distributions for the LHC, *Eur. Phys. J. C* 63 (2009) 189, arXiv:0901.0002 [hep-ph].
- [68] ATLAS Collaboration, Summary of ATLAS Pythia 8 tunes, ATL-PHYS-PUB-2012-003, <http://cds.cern.ch/record/1474107>, 2011.
- [69] G. Cowan, K. Cranmer, E. Gross, O. Vitells, Asymptotic formulae for likelihood-based tests of new physics, *Eur. Phys. J. C* 71 (2011) 1554, Erratum: *Eur. Phys. J. C* 73 (2013) 2501, arXiv:1007.1727 [physics.data-an].
- [70] A.L. Read, Presentation of search results: the CL(s) technique, *J. Phys. G* 28 (2002) 2693.
- [71] ATLAS Collaboration, Observation and measurement of Higgs boson decays to WW^* with the ATLAS detector, *Phys. Rev. D* 92 (2015) 012006, arXiv:1412.2641 [hep-ex].
- [72] ATLAS Collaboration, Search for squarks and gluinos with the ATLAS detector in final states with jets and missing transverse momentum using 4.7 fb^{-1} of $\sqrt{s} = 7$ TeV proton-proton collision data, *Phys. Rev. D* 87 (2013) 012008, arXiv:1208.0949 [hep-ex].
- [73] CMS Collaboration, Search for new physics in the multijet and missing transverse momentum final state in proton-proton collisions at $\sqrt{s} = 8$ TeV, *J. High Energy Phys.* 06 (2014) 055, arXiv:1402.4770 [hep-ex].
- [74] CMS Collaboration, Search for new physics with jets and missing transverse momentum in pp collisions at $\sqrt{s} = 7$ TeV, *J. High Energy Phys.* 08 (2011) 155, arXiv:1106.4503 [hep-ex].
- [75] ATLAS Collaboration, Jet energy scale measurements and their systematic uncertainties in proton-proton collisions at $\sqrt{s} = 13$ TeV with the ATLAS detector, *Phys. Rev. D* 96 (2017) 072002, arXiv:1703.09665 [hep-ex].
- [76] ATLAS Collaboration, Performance of missing transverse momentum reconstruction with the ATLAS detector using proton-proton collisions at $\sqrt{s} = 13$ TeV, arXiv:1802.08168 [hep-ex], 2018.
- [77] ATLAS Collaboration, Luminosity determination in pp collisions at $\sqrt{s} = 8$ TeV using the ATLAS detector at the LHC, *Eur. Phys. J. C* 76 (2016) 653, arXiv:1608.03953 [hep-ex].
- [78] G. Avoni, et al., The new LUCID-2 detector for luminosity measurement and monitoring in ATLAS, *J. Instrum.* 13 (2018) P07017.
- [79] E. Bothmann, M. Schönerr, S. Schumann, Reweighting QCD matrix-element and parton-shower calculations, *Eur. Phys. J. C* 76 (2016) 590, arXiv:1606.08753 [hep-ph].
- [80] S. Dittmaier, C. Mariotti, G. Passarino, S. Heinemeyer, R. Tanaka (Eds.), Handbook of LHC Higgs Cross Sections: 3. Higgs Properties, 2013, Tech. Rep. CERN-2013-004, FERMILAB-CONF-13-667-T, arXiv:1307.1347 [hep-ph], 2013.
- [81] I.W. Stewart, F.J. Tackmann, Theory uncertainties for Higgs and other searches using jet bins, *Phys. Rev. D* 85 (2012) 034011, arXiv:1107.2117 [hep-ph].
- [82] B. Patt, F. Wilczek, Higgs-field portal into hidden sectors, MIT-CTP-3745, arXiv:hep-ph/0605188, 2006.
- [83] P.J. Fox, R. Harnik, J. Kopp, Y. Tsai, Missing energy signatures of dark matter at the LHC, *Phys. Rev. D* 85 (2012) 056011, arXiv:1109.4398 [hep-ph].
- [84] A. De Simone, G.F. Giudice, A. Strumia, Benchmarks for dark matter searches at the LHC, *J. High Energy Phys.* 06 (2014) 081, arXiv:1402.6287 [hep-ph].
- [85] D.S. Akerib, et al., Results from a search for dark matter in the complete LUX exposure, *Phys. Rev. Lett.* 118 (2017) 021303, arXiv:1608.07648 [astro-ph.CO].
- [86] X. Cui, et al., Dark matter results from 54-ton-day exposure of PandaX-II experiment, *Phys. Rev. Lett.* 119 (2017) 181302, arXiv:1708.06917 [astro-ph.CO].
- [87] E. Aprile, et al., Dark matter search results from a one tonne \times year exposure of XENON1T, arXiv:1805.12562 [astro-ph.CO], 2018.
- [88] M. Hoferichter, P. Klos, J. Menéndez, A. Schwenk, Improved limits for Higgs-portal dark matter from LHC searches, *Phys. Rev. Lett.* 119 (2017) 181803, arXiv:1708.02245 [hep-ph].

[89] S. Baek, P. Ko, W.-I. Park, Invisible Higgs decay width versus dark matter direct detection cross section in Higgs portal dark matter models, *Phys. Rev. D* 90 (2014) 055014, arXiv:1405.3530 [hep-ph].

[90] ATLAS Collaboration, ATLAS Computing Acknowledgements ATL-GEN-PUB-2016-002, <http://cds.cern.ch/record/2202407>, 2016.

The ATLAS Collaboration

M. Aaboud^{34d}, G. Aad⁹⁹, B. Abbott¹²⁵, O. Abdinov^{13,*}, B. Abeloos¹²⁹, D.K. Abhayasinghe⁹¹, S.H. Abidi¹⁶⁴, O.S. AbouZeid³⁹, N.L. Abraham¹⁵³, H. Abramowicz¹⁵⁸, H. Abreu¹⁵⁷, Y. Abulaiti⁶, B.S. Acharya^{64a,64b,o}, S. Adachi¹⁶⁰, L. Adamczyk^{81a}, J. Adelman¹¹⁹, M. Adersberger¹¹², A. Adiguzel^{12c,ah}, T. Adye¹⁴¹, A.A. Affolder¹⁴³, Y. Afik¹⁵⁷, C. Agheorghiesei^{27c}, J.A. Aguilar-Saavedra^{137f,137a}, F. Ahmadov^{77,af}, G. Aielli^{71a,71b}, S. Akatsuka⁸³, T.P.A. Åkesson⁹⁴, E. Akilli⁵², A.V. Akimov¹⁰⁸, G.L. Alberghi^{23b,23a}, J. Albert¹⁷³, P. Albicocco⁴⁹, M.J. Alconada Verzini⁸⁶, S. Alderweireldt¹¹⁷, M. Aleksa³⁵, I.N. Aleksandrov⁷⁷, C. Alexa^{27b}, T. Alexopoulos¹⁰, M. Alhroob¹²⁵, B. Ali¹³⁹, G. Alimonti^{66a}, J. Alison³⁶, S.P. Alkire¹⁴⁵, C. Allaire¹²⁹, B.M.M. Allbrooke¹⁵³, B.W. Allen¹²⁸, P.P. Allport²¹, A. Aloisio^{67a,67b}, A. Alonso³⁹, F. Alonso⁸⁶, C. Alpigiani¹⁴⁵, A.A. Alshehri⁵⁵, M.I. Alstaty⁹⁹, B. Alvarez Gonzalez³⁵, D. Álvarez Piqueras¹⁷¹, M.G. Alviggi^{67a,67b}, B.T. Amadio¹⁸, Y. Amaral Coutinho^{78b}, L. Ambroz¹³², C. Amelung²⁶, D. Amidei¹⁰³, S.P. Amor Dos Santos^{137a,137c}, S. Amoroso⁴⁴, C.S. Amrouche⁵², C. Anastopoulos¹⁴⁶, L.S. Ancu⁵², N. Andari²¹, T. Andeen¹¹, C.F. Anders^{59b}, J.K. Anders²⁰, K.J. Anderson³⁶, A. Andreazza^{66a,66b}, V. Andrei^{59a}, C.R. Anelli¹⁷³, S. Angelidakis³⁷, I. Angelozzi¹¹⁸, A. Angerami³⁸, A.V. Anisenkov^{120b,120a}, A. Annovi^{69a}, C. Antel^{59a}, M.T. Anthony¹⁴⁶, M. Antonelli⁴⁹, D.J.A. Antrim¹⁶⁸, F. Anulli^{70a}, M. Aoki⁷⁹, L. Aperio Bella³⁵, G. Arabidze¹⁰⁴, J.P. Araque^{137a}, V. Araujo Ferraz^{78b}, R. Araujo Pereira^{78b}, A.T.H. Arce⁴⁷, R.E. Ardell⁹¹, F.A. Arduh⁸⁶, J-F. Arguin¹⁰⁷, S. Argyropoulos⁷⁵, A.J. Armbruster³⁵, L.J. Armitage⁹⁰, A. Armstrong¹⁶⁸, O. Arnaez¹⁶⁴, H. Arnold¹¹⁸, M. Arratia³¹, O. Arslan²⁴, A. Artamonov^{109,*}, G. Artoni¹³², S. Artz⁹⁷, S. Asai¹⁶⁰, N. Asbah⁴⁴, A. Ashkenazi¹⁵⁸, E.M. Asimakopoulou¹⁶⁹, L. Asquith¹⁵³, K. Assamagan²⁹, R. Astalos^{28a}, R.J. Atkin^{32a}, M. Atkinson¹⁷⁰, N.B. Atlay¹⁴⁸, K. Augsten¹³⁹, G. Avolio³⁵, R. Avramidou^{58a}, M.K. Ayoub^{15a}, G. Azuelos^{107,au}, A.E. Baas^{59a}, M.J. Baca²¹, H. Bachacou¹⁴², K. Bachas^{65a,65b}, M. Backes¹³², P. Bagnaia^{70a,70b}, M. Bahmani⁸², H. Bahrasemani¹⁴⁹, A.J. Bailey¹⁷¹, J.T. Baines¹⁴¹, M. Bajic³⁹, C. Bakalis¹⁰, O.K. Baker¹⁸⁰, P.J. Bakker¹¹⁸, D. Bakshi Gupta⁹³, E.M. Baldin^{120b,120a}, P. Balek¹⁷⁷, F. Balli¹⁴², W.K. Balunas¹³⁴, J. Balz⁹⁷, E. Banas⁸², A. Bandyopadhyay²⁴, S. Banerjee^{178,k}, A.A.E. Bannoura¹⁷⁹, L. Barak¹⁵⁸, W.M. Barbe³⁷, E.L. Barberio¹⁰², D. Barberis^{53b,53a}, M. Barbero⁹⁹, T. Barillari¹¹³, M-S. Barisits³⁵, J. Barkeloo¹²⁸, T. Barklow¹⁵⁰, N. Barlow³¹, R. Barnea¹⁵⁷, S.L. Barnes^{58c}, B.M. Barnett¹⁴¹, R.M. Barnett¹⁸, Z. Barnovska-Blenessy^{58a}, A. Baroncelli^{72a}, G. Barone²⁶, A.J. Barr¹³², L. Barranco Navarro¹⁷¹, F. Barreiro⁹⁶, J. Barreiro Guimarães da Costa^{15a}, R. Bartoldus¹⁵⁰, A.E. Barton⁸⁷, P. Bartos^{28a}, A. Basalae¹³⁵, A. Bassalat¹²⁹, R.L. Bates⁵⁵, S.J. Batista¹⁶⁴, S. Batlamous^{34e}, J.R. Batley³¹, M. Battaglia¹⁴³, M. Bauge^{70a,70b}, F. Bauer¹⁴², K.T. Bauer¹⁶⁸, H.S. Bawa^{150,m}, J.B. Beacham¹²³, M.D. Beattie⁸⁷, T. Beau¹³³, P.H. Beauchemin¹⁶⁷, P. Bechtel²⁴, H.C. Beck⁵¹, H.P. Beck^{20,r}, K. Becker⁵⁰, M. Becker⁹⁷, C. Becot⁴⁴, A. Beddall^{12d}, A.J. Beddall^{12a}, V.A. Bednyakov⁷⁷, M. Bedognetti¹¹⁸, C.P. Bee¹⁵², T.A. Beermann³⁵, M. Begalli^{78b}, M. Begel²⁹, A. Behera¹⁵², J.K. Behr⁴⁴, A.S. Bell⁹², G. Bella¹⁵⁸, L. Bellagamba^{23b}, A. Bellerive³³, M. Bellomo¹⁵⁷, P. Bellos⁹, K. Belotskiy¹¹⁰, N.L. Belyaev¹¹⁰, O. Benary^{158,*}, D. Benchekroun^{34a}, M. Bender¹¹², N. Benekos¹⁰, Y. Benhammou¹⁵⁸, E. Benhar Nocchioli¹⁸⁰, J. Benitez⁷⁵, D.P. Benjamin⁴⁷, M. Benoit⁵², J.R. Bensinger²⁶, S. Bentvelsen¹¹⁸, L. Beresford¹³², M. Beretta⁴⁹, D. Berge⁴⁴, E. Bergeaas Kuutmann¹⁶⁹, N. Berger⁵, L.J. Bergsten²⁶, J. Beringer¹⁸, S. Berlendis⁷, N.R. Bernard¹⁰⁰, G. Bernardi¹³³, C. Bernius¹⁵⁰, F.U. Bernlochner²⁴, T. Berry⁹¹, P. Berta⁹⁷, C. Bertella^{15a}, G. Bertoli^{43a,43b}, I.A. Bertram⁸⁷, G.J. Besjes³⁹, O. Bessidskaia Bylund^{43a,43b}, M. Bessner⁴⁴, N. Besson¹⁴², A. Bethani⁹⁸, S. Bethke¹¹³, A. Betti²⁴, A.J. Bevan⁹⁰, J. Beyer¹¹³, R.M. Bianchi¹³⁶, O. Biebel¹¹², D. Biedermann¹⁹, R. Bielski⁹⁸, K. Bierwagen⁹⁷, N.V. Biesuz^{69a,69b}, M. Biglietti^{72a}, T.R.V. Billoud¹⁰⁷, M. Bindi⁵¹, A. Bingul^{12d}, C. Bini^{70a,70b}, S. Biondi^{23b,23a}, M. Birman¹⁷⁷, T. Bisanz⁵¹, J.P. Biswal¹⁵⁸, C. Bittrich⁴⁶, D.M. Bjergaard⁴⁷, J.E. Black¹⁵⁰, K.M. Black²⁵, T. Blazek^{28a}, I. Bloch⁴⁴, C. Blocker²⁶, A. Blue⁵⁵, U. Blumenschein⁹⁰, Dr. Blunier^{144a}, G.J. Bobbink¹¹⁸, V.S. Bobrovnikov^{120b,120a}, S.S. Bocchetta⁹⁴, A. Bocci⁴⁷, D. Boerner¹⁷⁹, D. Bogavac¹¹², A.G. Bogdanchikov^{120b,120a}, C. Bohm^{43a}, V. Boisvert⁹¹, P. Bokan¹⁶⁹, T. Bold^{81a}, A.S. Boldyrev¹¹¹, A.E. Bolz^{59b}, M. Bomben¹³³, M. Bona⁹⁰, J.S. Bonilla¹²⁸, M. Boonekamp¹⁴², A. Borisov¹²¹, G. Borissov⁸⁷, J. Bortfeldt³⁵, D. Bortoletto¹³², V. Bortolotto^{71a,61b,61c,71b}, D. Boscherini^{23b}, M. Bosman¹⁴, J.D. Bossio Sola³⁰, K. Bouaouda^{34a}, J. Boudreau¹³⁶, E.V. Bouhova-Thacker⁸⁷, D. Boumediene³⁷,

C. Bourdarios¹²⁹, S.K. Boutle⁵⁵, A. Boveia¹²³, J. Boyd³⁵, I.R. Boyko⁷⁷, A.J. Bozson⁹¹, J. Bracinik²¹, N. Brahimi⁹⁹, A. Brandt⁸, G. Brandt¹⁷⁹, O. Brandt^{59a}, F. Braren⁴⁴, U. Bratzler¹⁶¹, B. Brau¹⁰⁰, J.E. Brau¹²⁸, W.D. Breaden Madden⁵⁵, K. Brendlinger⁴⁴, A.J. Brennan¹⁰², L. Brenner⁴⁴, R. Brenner¹⁶⁹, S. Bressler¹⁷⁷, B. Brickwedde⁹⁷, D.L. Briglin²¹, D. Britton⁵⁵, D. Britzger^{59b}, I. Brock²⁴, R. Brock¹⁰⁴, G. Brooijmans³⁸, T. Brooks⁹¹, W.K. Brooks^{144b}, E. Brost¹¹⁹, J.H. Broughton²¹, P.A. Bruckman de Renstrom⁸², D. Bruncko^{28b}, A. Bruni^{23b}, G. Bruni^{23b}, L.S. Bruni¹¹⁸, S. Bruno^{71a,71b}, B.H. Brunt³¹, M. Bruschi^{23b}, N. Brusino¹³⁶, P. Bryant³⁶, L. Bryngemark⁴⁴, T. Buanes¹⁷, Q. Buat³⁵, P. Buchholz¹⁴⁸, A.G. Buckley⁵⁵, I.A. Budagov⁷⁷, M.K. Bugge¹³¹, F. Bühner⁵⁰, O. Bulekov¹¹⁰, D. Bullock⁸, T.J. Burch¹¹⁹, S. Burdin⁸⁸, C.D. Burgard¹¹⁸, A.M. Burger⁵, B. Burghgrave¹¹⁹, K. Burka⁸², S. Burke¹⁴¹, I. Burmeister⁴⁵, J.T.P. Burr¹³², D. Büscher⁵⁰, V. Büscher⁹⁷, E. Buschmann⁵¹, P. Bussey⁵⁵, J.M. Butler²⁵, C.M. Buttar⁵⁵, J.M. Butterworth⁹², P. Butti³⁵, W. Buttinger³⁵, A. Buzatu¹⁵⁵, A.R. Buzykaev^{120b,120a}, G. Cabras^{23b,23a}, S. Cabrera Urbán¹⁷¹, D. Caforio¹³⁹, H. Cai¹⁷⁰, V.M.M. Cairo², O. Cakir^{4a}, N. Calace⁵², P. Calafiura¹⁸, A. Calandri⁹⁹, G. Calderini¹³³, P. Calfayan⁶³, G. Callea^{40b,40a}, L.P. Caloba^{78b}, S. Calvente Lopez⁹⁶, D. Calvet³⁷, S. Calvet³⁷, T.P. Calvet¹⁵², M. Calvetti^{69a,69b}, R. Camacho Toro¹³³, S. Camarda³⁵, P. Camarri^{71a,71b}, D. Cameron¹³¹, R. Caminal Armadans¹⁰⁰, C. Camincher³⁵, S. Campana³⁵, M. Campanelli⁹², A. Camplani³⁹, A. Campoverde¹⁴⁸, V. Canale^{67a,67b}, M. Cano Bret^{58c}, J. Cantero¹²⁶, T. Cao¹⁵⁸, Y. Cao¹⁷⁰, M.D.M. Capeans Garrido³⁵, I. Caprini^{27b}, M. Caprini^{27b}, M. Capua^{40b,40a}, R.M. Carbone³⁸, R. Cardarelli^{71a}, F.C. Cardillo⁵⁰, I. Carli¹⁴⁰, T. Carli³⁵, G. Carlino^{67a}, B.T. Carlson¹³⁶, L. Carminati^{66a,66b}, R.M.D. Carney^{43a,43b}, S. Caron¹¹⁷, E. Carquin^{144b}, S. Carrá^{66a,66b}, G.D. Carrillo-Montoya³⁵, D. Casadei^{32b}, M.P. Casado^{14g}, A.F. Casha¹⁶⁴, M. Casolino¹⁴, D.W. Casper¹⁶⁸, R. Castelijns¹¹⁸, F.L. Castillo¹⁷¹, V. Castillo Gimenez¹⁷¹, N.F. Castro^{137a,137e}, A. Catinaccio³⁵, J.R. Catmore¹³¹, A. Cattai³⁵, J. Caudron²⁴, V. Cavaliere²⁹, E. Cavallaro¹⁴, D. Cavalli^{66a}, M. Cavalli-Sforza¹⁴, V. Cavasinni^{69a,69b}, E. Celebi^{12b}, F. Ceradini^{72a,72b}, L. Cerda Alberich¹⁷¹, A.S. Cerqueira^{78a}, A. Cerri¹⁵³, L. Cerrito^{71a,71b}, F. Cerutti¹⁸, A. Cervelli^{23b,23a}, S.A. Cetin^{12b}, A. Chafaq^{34a}, D. Chakraborty¹¹⁹, S.K. Chan⁵⁷, W.S. Chan¹¹⁸, Y.L. Chan^{61a}, J.D. Chapman³¹, D.G. Charlton²¹, C.C. Chau³³, C.A. Chavez Barajas¹⁵³, S. Che¹²³, A. Chegwiddden¹⁰⁴, S. Chekanov⁶, S.V. Chekulaev^{165a}, G.A. Chelkov^{77,at}, M.A. Chelstowska³⁵, C. Chen^{58a}, C.H. Chen⁷⁶, H. Chen²⁹, J. Chen^{58a}, J. Chen³⁸, S. Chen¹³⁴, S.J. Chen^{15c}, X. Chen^{15b,as}, Y. Chen⁸⁰, Y.-H. Chen⁴⁴, H.C. Cheng¹⁰³, H.J. Cheng^{15d}, A. Cheplakov⁷⁷, E. Cheremushkina¹²¹, R. Cherkaoui El Moursli^{34e}, E. Cheu⁷, K. Cheung⁶², L. Chevalier¹⁴², V. Chiarella⁴⁹, G. Chiarelli^{69a}, G. Chiodini^{65a}, A.S. Chisholm³⁵, A. Chitan^{27b}, I. Chiu¹⁶⁰, Y.H. Chiu¹⁷³, M.V. Chizhov⁷⁷, K. Choi⁶³, A.R. Chomont¹²⁹, S. Chouridou¹⁵⁹, Y.S. Chow¹¹⁸, V. Christodoulou⁹², M.C. Chu^{61a}, J. Chudoba¹³⁸, A.J. Chuinard¹⁰¹, J.J. Chwastowski⁸², L. Chytka¹²⁷, D. Cinca⁴⁵, V. Cindro⁸⁹, I.A. Cioarǎ²⁴, A. Ciocio¹⁸, F. Ciotto^{67a,67b}, Z.H. Citron¹⁷⁷, M. Citterio^{66a}, A. Clark⁵², M.R. Clark³⁸, P.J. Clark⁴⁸, C. Clement^{43a,43b}, Y. Coadou⁹⁹, M. Cobal^{64a,64c}, A. Coccaro^{53b,53a}, J. Cochran⁷⁶, A.E.C. Coimbra¹⁷⁷, L. Colasurdo¹¹⁷, B. Cole³⁸, A.P. Colijn¹¹⁸, J. Collot⁵⁶, P. Conde Muiño^{137a,137b}, E. Coniavitis⁵⁰, S.H. Connell^{32b}, I.A. Connelly⁹⁸, S. Constantinescu^{27b}, F. Conventi^{67a,av}, A.M. Cooper-Sarkar¹³², F. Cormier¹⁷², K.J.R. Cormier¹⁶⁴, M. Corradi^{70a,70b}, E.E. Corrigan⁹⁴, F. Corriveau^{101,ad}, A. Cortes-Gonzalez³⁵, M.J. Costa¹⁷¹, D. Costanzo¹⁴⁶, G. Cottin³¹, G. Cowan⁹¹, B.E. Cox⁹⁸, J. Crane⁹⁸, K. Cranmer¹²², S.J. Crawley⁵⁵, R.A. Creager¹³⁴, G. Cree³³, S. Crépé-Renaudin⁵⁶, F. Crescioli¹³³, M. Cristinziani²⁴, V. Croft¹²², G. Crosetti^{40b,40a}, A. Cueto⁹⁶, T. Cuhadar Donszelmann¹⁴⁶, A.R. Cukierman¹⁵⁰, J. Cúth⁹⁷, S. Czekierda⁸², P. Czodrowski³⁵, M.J. Da Cunha Sargedas De Sousa^{58b}, C. Da Via⁹⁸, W. Dabrowski^{81a}, T. Dado^{28a,y}, S. Dahbi^{34e}, T. Dai¹⁰³, F. Dallaire¹⁰⁷, C. Dallapiccola¹⁰⁰, M. Dam³⁹, G. D'amen^{23b,23a}, J. Damp⁹⁷, J.R. Dandoy¹³⁴, M.F. Daneri³⁰, N.P. Dang^{178,k}, N.D. Dann⁹⁸, M. Danninger¹⁷², V. Dao³⁵, G. Darbo^{53b}, S. Darmora⁸, O. Dartsis⁵, A. Dattagupta¹²⁸, T. Daubney⁴⁴, S. D'Auria⁵⁵, W. Davey²⁴, C. David⁴⁴, T. Davidek¹⁴⁰, D.R. Davis⁴⁷, E. Dawe¹⁰², I. Dawson¹⁴⁶, K. De⁸, R. De Asmundis^{67a}, A. De Benedetti¹²⁵, M. De Beurs¹¹⁸, S. De Castro^{23b,23a}, S. De Cecco^{70a,70b}, N. De Groot¹¹⁷, P. de Jong¹¹⁸, H. De la Torre¹⁰⁴, F. De Lorenzi⁷⁶, A. De Maria^{51,t}, D. De Pedis^{70a}, A. De Salvo^{70a}, U. De Sanctis^{71a,71b}, A. De Santo¹⁵³, K. De Vasconcelos Corga⁹⁹, J.B. De Vivie De Regie¹²⁹, C. Debenedetti¹⁴³, D.V. Dedovich⁷⁷, N. Dehghanian³, M. Del Gaudio^{40b,40a}, J. Del Peso⁹⁶, Y. Delabat Diaz⁴⁴, D. Delgove¹²⁹, F. Deliot¹⁴², C.M. Delitzsch⁷, M. Della Pietra^{67a,67b}, D. Della Volpe⁵², A. Dell'Acqua³⁵, L. Dell'Asta²⁵, M. Delmastro⁵, C. Delporte¹²⁹, P.A. Delsart⁵⁶, D.A. DeMarco¹⁶⁴, S. Demers¹⁸⁰, M. Demichev⁷⁷, S.P. Denisov¹²¹, D. Denysiuk¹¹⁸, L. D'Eramo¹³³, D. Derendarz⁸², J.E. Derkaoui^{34d}, F. Derue¹³³, P. Dervan⁸⁸, K. Desch²⁴,

C. Deterre⁴⁴, K. Dette¹⁶⁴, M.R. Devesa³⁰, P.O. Deviveiros³⁵, A. Dewhurst¹⁴¹, S. Dhaliwal²⁶, F.A. Di Bello⁵², A. Di Ciaccio^{71a,71b}, L. Di Ciaccio⁵, W.K. Di Clemente¹³⁴, C. Di Donato^{67a,67b}, A. Di Girolamo³⁵, B. Di Micco^{72a,72b}, R. Di Nardo¹⁰⁰, K.F. Di Petrillo⁵⁷, A. Di Simone⁵⁰, R. Di Sipio¹⁶⁴, D. Di Valentino³³, C. Diaconu⁹⁹, M. Diamond¹⁶⁴, F.A. Dias³⁹, T. Dias Do Vale^{137a}, M.A. Diaz^{144a}, J. Dickinson¹⁸, E.B. Diehl¹⁰³, J. Dietrich¹⁹, S. Díez Cornell⁴⁴, A. Dimitrievska¹⁸, J. Dingfelder²⁴, F. Dittus³⁵, F. Djama⁹⁹, T. Djobava^{156b}, J.I. Djuvsland^{59a}, M.A.B. Do Vale^{78c}, M. Dobre^{27b}, D. Dodsworth²⁶, C. Doglioni⁹⁴, J. Dolejsi¹⁴⁰, Z. Dolezal¹⁴⁰, M. Donadelli^{78d}, J. Donini³⁷, A. D'Onofrio⁹⁰, M. D'Onofrio⁸⁸, J. Dopke¹⁴¹, A. Doria^{67a}, M.T. Dova⁸⁶, A.T. Doyle⁵⁵, E. Drechsler⁵¹, E. Dreyer¹⁴⁹, T. Dreyer⁵¹, Y. Du^{58b}, J. Duarte-Campderros¹⁵⁸, F. Dubinin¹⁰⁸, M. Dubovsky^{28a}, A. Dubreuil⁵², E. Duchovni¹⁷⁷, G. Duckeck¹¹², A. Ducourthial¹³³, O.A. Ducu^{107,x}, D. Duda¹¹³, A. Dudarev³⁵, A.C. Dudder⁹⁷, E.M. Duffield¹⁸, L. Dufлот¹²⁹, M. Dührssen³⁵, C. Dülsen¹⁷⁹, M. Dumancic¹⁷⁷, A.E. Dumitriu^{27b,e}, A.K. Duncan⁵⁵, M. Dunford^{59a}, A. Duperrin⁹⁹, H. Duran Yildiz^{4a}, M. Düren⁵⁴, A. Durglishvili^{156b}, D. Duschinger⁴⁶, B. Dutta⁴⁴, D. Duvnjak¹, M. Dyndal⁴⁴, S. Dysch⁹⁸, B.S. Dziejczak⁸², C. Eckardt⁴⁴, K.M. Ecker¹¹³, R.C. Edgar¹⁰³, T. Eifert³⁵, G. Eigen¹⁷, K. Einsweiler¹⁸, T. Ekelof¹⁶⁹, M. El Kacimi^{34c}, R. El Kosseifi⁹⁹, V. Ellajosyula⁹⁹, M. Ellert¹⁶⁹, F. Ellinghaus¹⁷⁹, A.A. Elliot⁹⁰, N. Ellis³⁵, J. Elmsheuser²⁹, M. Elsing³⁵, D. Emelianov¹⁴¹, Y. Enari¹⁶⁰, J.S. Ennis¹⁷⁵, M.B. Epland⁴⁷, J. Erdmann⁴⁵, A. Ereditato²⁰, S. Errede¹⁷⁰, M. Escalier¹²⁹, C. Escobar¹⁷¹, O. Estrada Pastor¹⁷¹, A.I. Etienne¹⁴², E. Etzion¹⁵⁸, H. Evans⁶³, A. Ezhilov¹³⁵, M. Ezzi^{34e}, F. Fabbri⁵⁵, L. Fabbri^{23b,23a}, V. Fabiani¹¹⁷, G. Facini⁹², R.M. Faisca Rodrigues Pereira^{137a}, R.M. Fakhruddinov¹²¹, S. Falciano^{70a}, P.J. Falke⁵, S. Falke⁵, J. Faltova¹⁴⁰, Y. Fang^{15a}, M. Fanti^{66a,66b}, A. Farbin⁸, A. Farilla^{72a}, E.M. Farina^{68a,68b}, T. Farooque¹⁰⁴, S. Farrell¹⁸, S.M. Farrington¹⁷⁵, P. Farthouat³⁵, F. Fassi^{34e}, P. Fassnacht³⁵, D. Fassouliotis⁹, M. Fauci Giannelli⁴⁸, A. Favareto^{53b,53a}, W.J. Fawcett⁵², L. Fayard¹²⁹, O.L. Fedin^{135,p}, W. Fedorko¹⁷², M. Feickert⁴¹, S. Feigl¹³¹, L. Feligioni⁹⁹, C. Feng^{58b}, E.J. Feng³⁵, M. Feng⁴⁷, M.J. Fenton⁵⁵, A.B. Fenyuk¹²¹, L. Feremenga⁸, J. Ferrando⁴⁴, A. Ferrari¹⁶⁹, P. Ferrari¹¹⁸, R. Ferrari^{68a}, D.E. Ferreira de Lima^{59b}, A. Ferrer¹⁷¹, D. Ferrere⁵², C. Ferretti¹⁰³, F. Fiedler⁹⁷, A. Filipčič⁸⁹, F. Filthaut¹¹⁷, K.D. Finelli²⁵, M.C.N. Fiolhais^{137a,137c,a}, L. Fiorini¹⁷¹, C. Fischer¹⁴, W.C. Fisher¹⁰⁴, N. Flaschel⁴⁴, I. Fleck¹⁴⁸, P. Fleischmann¹⁰³, R.R.M. Fletcher¹³⁴, T. Flick¹⁷⁹, B.M. Flierl¹¹², L.M. Flores¹³⁴, L.R. Flores Castillo^{61a}, N. Fomin¹⁷, G.T. Forcolin⁹⁸, A. Formica¹⁴², F.A. Förster¹⁴, A.C. Forti⁹⁸, A.G. Foster²¹, D. Fournier¹²⁹, H. Fox⁸⁷, S. Fracchia¹⁴⁶, P. Francavilla^{69a,69b}, M. Franchini^{23b,23a}, S. Franchino^{59a}, D. Francis³⁵, L. Franconi¹³¹, M. Franklin⁵⁷, M. Frate¹⁶⁸, M. Fraternali^{68a,68b}, D. Freeborn⁹², S.M. Fressard-Batranceanu³⁵, B. Freund¹⁰⁷, W.S. Freund^{78b}, D. Froidevaux³⁵, J.A. Frost¹³², C. Fukunaga¹⁶¹, E. Fullana Torregrosa¹⁷¹, T. Fusayasu¹¹⁴, J. Fuster¹⁷¹, O. Gabizon¹⁵⁷, A. Gabrielli^{23b,23a}, A. Gabrielli¹⁸, G.P. Gach^{81a}, S. Gadatsch⁵², P. Gadow¹¹³, G. Gagliardi^{53b,53a}, L.G. Gagnon¹⁰⁷, C. Galea^{27b}, B. Galhardo^{137a,137c}, E.J. Gallas¹³², B.J. Gallop¹⁴¹, P. Gallus¹³⁹, G. Galster³⁹, R. Gamboa Goni⁹⁰, K.K. Gan¹²³, S. Ganguly¹⁷⁷, Y. Gao⁸⁸, Y.S. Gao^{150,m}, C. García¹⁷¹, J.E. García Navarro¹⁷¹, J.A. García Pascual^{15a}, M. Garcia-Sciveres¹⁸, R.W. Gardner³⁶, N. Garelli¹⁵⁰, V. Garonne¹³¹, K. Gasnikova⁴⁴, A. Gaudiello^{53b,53a}, G. Gaudio^{68a}, I.L. Gavrilenko¹⁰⁸, A. Gavrilyuk¹⁰⁹, C. Gay¹⁷², G. Gaycken²⁴, E.N. Gazis¹⁰, C.N.P. Gee¹⁴¹, J. Geisen⁵¹, M. Geisen⁹⁷, M.P. Geisler^{59a}, K. Gellerstedt^{43a,43b}, C. Gemme^{53b}, M.H. Genest⁵⁶, C. Geng¹⁰³, S. Gentile^{70a,70b}, C. Gentsos¹⁵⁹, S. George⁹¹, D. Gerbaudo¹⁴, G. Gessner⁴⁵, S. Ghasemi¹⁴⁸, M. Ghasemi Bostanabad¹⁷³, M. Ghneimat²⁴, B. Giacobbe^{23b}, S. Giagu^{70a,70b}, N. Giangiacomi^{23b,23a}, P. Giannetti^{69a}, A. Giannini^{67a,67b}, S.M. Gibson⁹¹, M. Gignac¹⁴³, D. Gillberg³³, G. Gilles¹⁷⁹, D.M. Gingrich^{3,au}, M.P. Giordani^{64a,64c}, F.M. Giorgi^{23b}, P.F. Giraud¹⁴², P. Giromini⁵⁷, G. Giugliarelli^{64a,64c}, D. Giugni^{66a}, F. Giuli¹³², M. Giulini^{59b}, S. Gkaitatzis¹⁵⁹, I. Gkialas^{9,j}, E.L. Gkougkousis¹⁴, P. Gkoutoumis¹⁰, L.K. Gladilin¹¹¹, C. Glasman⁹⁶, J. Glatzer¹⁴, P.C.F. Glaysher⁴⁴, A. Glazov⁴⁴, M. Goblirsch-Kolb²⁶, J. Godlewski⁸², S. Goldfarb¹⁰², T. Golling⁵², D. Golubkov¹²¹, A. Gomes^{137a,137b,137d}, R. Goncalves Gama^{78a}, R. Gonçalves^{137a}, G. Gonella⁵⁰, L. Gonella²¹, A. Gongadze⁷⁷, F. Gonnella²¹, J.L. Gonski⁵⁷, S. González de la Hoz¹⁷¹, S. Gonzalez-Sevilla⁵², L. Goossens³⁵, P.A. Gorbounov¹⁰⁹, H.A. Gordon²⁹, B. Gorini³⁵, E. Gorini^{65a,65b}, A. Gorišek⁸⁹, A.T. Goshaw⁴⁷, C. Gössling⁴⁵, M.I. Gostkin⁷⁷, C.A. Gottardo²⁴, C.R. Goudet¹²⁹, D. Goujdami^{34c}, A.G. Goussiou¹⁴⁵, N. Govender^{32b,c}, C. Goy⁵, E. Gozani¹⁵⁷, I. Grabowska-Bold^{81a}, P.O.J. Gradin¹⁶⁹, E.C. Graham⁸⁸, J. Gramling¹⁶⁸, E. Gramstad¹³¹, S. Grancagnolo¹⁹, V. Gratchev¹³⁵, P.M. Gravila^{27f}, C. Gray⁵⁵, H.M. Gray¹⁸, Z.D. Greenwood^{93,aj}, C. Greife²⁴, K. Gregersen⁹², I.M. Gregor⁴⁴, P. Grenier¹⁵⁰, K. Grevtsov⁴⁴, J. Griffiths⁸, A.A. Grillo¹⁴³, K. Grimm^{150,b}, S. Grinstein^{14,z}, Ph. Gris³⁷, J.-F. Grivaz¹²⁹,

S. Groh⁹⁷, E. Gross¹⁷⁷, J. Grosse-Knetter⁵¹, G.C. Grossi⁹³, Z.J. Grout⁹², C. Grud¹⁰³, A. Grummer¹¹⁶, L. Guan¹⁰³, W. Guan¹⁷⁸, J. Guenther³⁵, A. Guerguichon¹²⁹, F. Guescini^{165a}, D. Guest¹⁶⁸, R. Gugel⁵⁰, B. Gui¹²³, T. Guillemin⁵, S. Guindon³⁵, U. Gul⁵⁵, C. Gumpert³⁵, J. Guo^{58c}, W. Guo¹⁰³, Y. Guo^{58a,s}, Z. Guo⁹⁹, R. Gupta⁴¹, S. Gurbuz^{12c}, G. Gustavino¹²⁵, B.J. Gutelman¹⁵⁷, P. Gutierrez¹²⁵, C. Gutschow⁹², C. Guyot¹⁴², M.P. Guzik^{81a}, C. Gwenlan¹³², C.B. Gwilliam⁸⁸, A. Haas¹²², C. Haber¹⁸, H.K. Hadavand⁸, N. Haddad^{34e}, A. Hadeef^{58a}, S. Hageböck²⁴, M. Hagihara¹⁶⁶, H. Hakobyan^{181,*}, M. Haleem¹⁷⁴, J. Haley¹²⁶, G. Halladjian¹⁰⁴, G.D. Hallewell⁹⁹, K. Hamacher¹⁷⁹, P. Hamal¹²⁷, K. Hamano¹⁷³, A. Hamilton^{32a}, G.N. Hamity¹⁴⁶, K. Han^{58a,ai}, L. Han^{58a}, S. Han^{15d}, K. Hanagaki^{79,v}, M. Hance¹⁴³, D.M. Handl¹¹², B. Haney¹³⁴, R. Hankache¹³³, P. Hanke^{59a}, E. Hansen⁹⁴, J.B. Hansen³⁹, J.D. Hansen³⁹, M.C. Hansen²⁴, P.H. Hansen³⁹, K. Hara¹⁶⁶, A.S. Hard¹⁷⁸, T. Harenberg¹⁷⁹, S. Harkusha¹⁰⁵, P.F. Harrison¹⁷⁵, N.M. Hartmann¹¹², Y. Hasegawa¹⁴⁷, A. Hasib⁴⁸, S. Hassani¹⁴², S. Haug²⁰, R. Hauser¹⁰⁴, L. Hauswald⁴⁶, L.B. Havener³⁸, M. Havranek¹³⁹, C.M. Hawkes²¹, R.J. Hawking³⁵, D. Hayden¹⁰⁴, C. Hayes¹⁵², C.P. Hays¹³², J.M. Hays⁹⁰, H.S. Hayward⁸⁸, S.J. Haywood¹⁴¹, M.P. Heath⁴⁸, V. Hedberg⁹⁴, L. Heelan⁸, S. Heer²⁴, K.K. Heidegger⁵⁰, J. Heilman³³, S. Heim⁴⁴, T. Heim¹⁸, B. Heinemann^{44,ap}, J.J. Heinrich¹¹², L. Heinrich¹²², C. Heinz⁵⁴, J. Hejbal¹³⁸, L. Helary³⁵, A. Held¹⁷², S. Hellesund¹³¹, S. Hellman^{43a,43b}, C. Hensens³⁵, R.C.W. Henderson⁸⁷, Y. Heng¹⁷⁸, S. Henkelmann¹⁷², A.M. Henriques Correia³⁵, G.H. Herbert¹⁹, H. Herde²⁶, V. Herget¹⁷⁴, Y. Hernández Jiménez^{32c}, H. Herr⁹⁷, M.G. Herrmann¹¹², G. Herten⁵⁰, R. Hertenberger¹¹², L. Hervas³⁵, T.C. Herwig¹³⁴, G.G. Hesketh⁹², N.P. Hessey^{165a}, J.W. Hetherly⁴¹, S. Higashino⁷⁹, E. Higón-Rodríguez¹⁷¹, K. Hildebrand³⁶, E. Hill¹⁷³, J.C. Hill³¹, K.K. Hill²⁹, K.H. Hiller⁴⁴, S.J. Hillier²¹, M. Hils⁴⁶, I. Hinchliffe¹⁸, M. Hirose¹³⁰, D. Hirschbuehl¹⁷⁹, B. Hiti⁸⁹, O. Hladik¹³⁸, D.R. Hlaluku^{32c}, X. Hoad⁴⁸, J. Hobbs¹⁵², N. Hod^{165a}, M.C. Hodgkinson¹⁴⁶, A. Hoecker³⁵, M.R. Hoferkamp¹¹⁶, F. Hoenig¹¹², D. Hohn²⁴, D. Hohov¹²⁹, T.R. Holmes³⁶, M. Holzbock¹¹², M. Homann⁴⁵, S. Honda¹⁶⁶, T. Honda⁷⁹, T.M. Hong¹³⁶, A. Hönle¹¹³, B.H. Hooberman¹⁷⁰, W.H. Hopkins¹²⁸, Y. Horii¹¹⁵, P. Horn⁴⁶, A.J. Horton¹⁴⁹, L.A. Horyn³⁶, J.-Y. Hostachy⁵⁶, A. Hostiuc¹⁴⁵, S. Hou¹⁵⁵, A. Hoummada^{34a}, J. Howarth⁹⁸, J. Hoya⁸⁶, M. Hrabovsky¹²⁷, J. Hrdinka³⁵, I. Hristova¹⁹, J. Hrivnac¹²⁹, A. Hrynevich¹⁰⁶, T. Hryn'ova⁵, P.J. Hsu⁶², S.-C. Hsu¹⁴⁵, Q. Hu²⁹, S. Hu^{58c}, Y. Huang^{15a}, Z. Hubacek¹³⁹, F. Hubaut⁹⁹, M. Huebner²⁴, F. Huegging²⁴, T.B. Huffman¹³², E.W. Hughes³⁸, M. Huhtinen³⁵, R.F.H. Hunter³³, P. Huo¹⁵², A.M. Hupe³³, N. Huseynov^{77,af}, J. Huston¹⁰⁴, J. Huth⁵⁷, R. Hyneman¹⁰³, G. Iacobucci⁵², G. Iakovidis²⁹, I. Ibragimov¹⁴⁸, L. Iconomidou-Fayard¹²⁹, Z. Idrissi^{34e}, P. Iengo³⁵, R. Ignazzi³⁹, O. Igonkina^{118,ab}, R. Iguchi¹⁶⁰, T. Iizawa⁵², Y. Ikegami⁷⁹, M. Ikeno⁷⁹, D. Iliadis¹⁵⁹, N. Ilic¹⁵⁰, F. Iltzsche⁴⁶, G. Introzzi^{68a,68b}, M. Iodice^{72a}, K. Iordanidou³⁸, V. Ippolito^{70a,70b}, M.F. Isacson¹⁶⁹, N. Ishijima¹³⁰, M. Ishino¹⁶⁰, M. Ishitsuka¹⁶², W. Islam¹²⁶, C. Issever¹³², S. Istin^{12c,ao}, F. Ito¹⁶⁶, J.M. Iturbe Ponce^{61a}, R. Iuppa^{73a,73b}, A. Ivina¹⁷⁷, H. Iwasaki⁷⁹, J.M. Izen⁴², V. Izzo^{67a}, S. Jabbar³, P. Jacka¹³⁸, P. Jackson¹, R.M. Jacobs²⁴, V. Jain², G. Jäkel¹⁷⁹, K.B. Jakobi⁹⁷, K. Jakobs⁵⁰, S. Jakobsen⁷⁴, T. Jakoubek¹³⁸, D.O. Jamin¹²⁶, D.K. Jana⁹³, R. Jansky⁵², J. Janssen²⁴, M. Janus⁵¹, P.A. Janus^{81a}, G. Jarlskog⁹⁴, N. Javadov^{77,af}, T. Javůrek⁵⁰, M. Javurkova⁵⁰, F. Jeanneau¹⁴², L. Jeanty¹⁸, J. Jejelava^{156a,ag}, A. Jelinskas¹⁷⁵, P. Jenni^{50,d}, J. Jeong⁴⁴, S. Jézéquel⁵, H. Ji¹⁷⁸, J. Jia¹⁵², H. Jiang⁷⁶, Y. Jiang^{58a}, Z. Jiang^{150,q}, S. Jiggins⁵⁰, F.A. Jimenez Morales³⁷, J. Jimenez Pena¹⁷¹, S. Jin^{15c}, A. Jinaru^{27b}, O. Jinnouchi¹⁶², H. Jivan^{32c}, P. Johansson¹⁴⁶, K.A. Johns⁷, C.A. Johnson⁶³, W.J. Johnson¹⁴⁵, K. Jon-And^{43a,43b}, R.W.L. Jones⁸⁷, S.D. Jones¹⁵³, S. Jones⁷, T.J. Jones⁸⁸, J. Jongmanns^{59a}, P.M. Jorge^{137a,137b}, J. Jovicevic^{165a}, X. Ju¹⁷⁸, J.J. Junggeburth¹¹³, A. Juste Rozas^{14,z}, A. Kaczmarska⁸², M. Kado¹²⁹, H. Kagan¹²³, M. Kagan¹⁵⁰, T. Kaji¹⁷⁶, E. Kajomovitz¹⁵⁷, C.W. Kalderon⁹⁴, A. Kaluza⁹⁷, S. Kama⁴¹, A. Kamenshchikov¹²¹, L. Kanjir⁸⁹, Y. Kano¹⁶⁰, V.A. Kantserov¹¹⁰, J. Kanzaki⁷⁹, B. Kaplan¹²², L.S. Kaplan¹⁷⁸, D. Kar^{32c}, M.J. Kareem^{165b}, E. Karentzos¹⁰, S.N. Karpov⁷⁷, Z.M. Karpova⁷⁷, V. Kartvelishvili⁸⁷, A.N. Karyukhin¹²¹, K. Kasahara¹⁶⁶, L. Kashif¹⁷⁸, R.D. Kass¹²³, A. Kastanas¹⁵¹, Y. Kataoka¹⁶⁰, C. Kato¹⁶⁰, J. Katzy⁴⁴, K. Kawade⁸⁰, K. Kawagoe⁸⁵, T. Kawamoto¹⁶⁰, G. Kawamura⁵¹, E.F. Kay⁸⁸, V.F. Kazanin^{120b,120a}, R. Keeler¹⁷³, R. Kehoe⁴¹, J.S. Keller³³, E. Kellermann⁹⁴, J.J. Kempster²¹, J. Kendrick²¹, O. Kepka¹³⁸, S. Kersten¹⁷⁹, B.P. Kerševan⁸⁹, R.A. Keyes¹⁰¹, M. Khader¹⁷⁰, F. Khalil-Zada¹³, A. Khanov¹²⁶, A.G. Kharlamov^{120b,120a}, T. Kharlamova^{120b,120a}, A. Khodinov¹⁶³, T.J. Khoo⁵², E. Khramov⁷⁷, J. Khubua^{156b}, S. Kido⁸⁰, M. Kiehn⁵², C.R. Kilby⁹¹, S.H. Kim¹⁶⁶, Y.K. Kim³⁶, N. Kimura^{64a,64c}, O.M. Kind¹⁹, B.T. King⁸⁸, D. Kirchmeier⁴⁶, J. Kirk¹⁴¹, A.E. Kiryunin¹¹³, T. Kishimoto¹⁶⁰, D. Kisielewska^{81a}, V. Kitali⁴⁴, O. Kivernyk⁵, E. Kladiva^{28b,*}, T. Klapdor-Kleingrothaus⁵⁰, M.H. Klein¹⁰³,

M. Klein⁸⁸, U. Klein⁸⁸, K. Kleinknecht⁹⁷, P. Klimek¹¹⁹, A. Klimentov²⁹, R. Klingenberg^{45,*}, T. Klingl²⁴, T. Klioutchnikova³⁵, F.F. Klitzner¹¹², P. Kluit¹¹⁸, S. Kluth¹¹³, E. Kneringer⁷⁴, E.B.F.G. Knoops⁹⁹, A. Knue⁵⁰, A. Kobayashi¹⁶⁰, D. Kobayashi⁸⁵, T. Kobayashi¹⁶⁰, M. Kobel⁴⁶, M. Kocian¹⁵⁰, P. Kodys¹⁴⁰, T. Koffas³³, E. Koffeman¹¹⁸, N.M. Köhler¹¹³, T. Koi¹⁵⁰, M. Kolb^{59b}, I. Koletsou⁵, T. Kondo⁷⁹, N. Kondrashova^{58c}, K. Köneke⁵⁰, A.C. König¹¹⁷, T. Kono⁷⁹, R. Konoplich^{122,al}, V. Konstantinides⁹², N. Konstantinidis⁹², B. Konya⁹⁴, R. Kopeliansky⁶³, S. Koperny^{81a}, K. Korcyl⁸², K. Kordas¹⁵⁹, A. Korn⁹², I. Korolkov¹⁴, E.V. Korolkova¹⁴⁶, O. Kortner¹¹³, S. Kortner¹¹³, T. Kosek¹⁴⁰, V.V. Kostyukhin²⁴, A. Kotwal⁴⁷, A. Koulouris¹⁰, A. Kourkoumeli-Charalampidi^{68a,68b}, C. Kourkoumelis⁹, E. Kourlitis¹⁴⁶, V. Kouskoura²⁹, A.B. Kowalewska⁸², R. Kowalewski¹⁷³, T.Z. Kowalski^{81a}, C. Kozakai¹⁶⁰, W. Kozanecki¹⁴², A.S. Kozhin¹²¹, V.A. Kramarenko¹¹¹, G. Kramberger⁸⁹, D. Krasnopevtsev¹¹⁰, M.W. Krasny¹³³, A. Krasznahorkay³⁵, D. Krauss¹¹³, J.A. Kremer^{81a}, J. Kretzschmar⁸⁸, P. Krieger¹⁶⁴, K. Krizka¹⁸, K. Kroeninger⁴⁵, H. Kroha¹¹³, J. Kroll¹³⁸, J. Kroll¹³⁴, J. Krstic¹⁶, U. Kruchonak⁷⁷, H. Krüger²⁴, N. Krumnack⁷⁶, M.C. Kruse⁴⁷, T. Kubota¹⁰², S. Kuday^{4b}, J.T. Kuechler¹⁷⁹, S. Kuehn³⁵, A. Kugel^{59a}, F. Kuger¹⁷⁴, T. Kuhl⁴⁴, V. Kukhtin⁷⁷, R. Kukla⁹⁹, Y. Kulchitsky¹⁰⁵, S. Kuleshov^{144b}, Y.P. Kulinich¹⁷⁰, M. Kuna⁵⁶, T. Kunigo⁸³, A. Kupco¹³⁸, T. Kupfer⁴⁵, O. Kuprash¹⁵⁸, H. Kurashige⁸⁰, L.L. Kurchaninov^{165a}, Y.A. Kurochkin¹⁰⁵, M.G. Kurth^{15d}, E.S. Kuwertz¹⁷³, M. Kuze¹⁶², J. Kvita¹²⁷, T. Kwan¹⁰¹, A. La Rosa¹¹³, J.L. La Rosa Navarro^{78d}, L. La Rotonda^{40b,40a}, F. La Ruffa^{40b,40a}, C. Lacasta¹⁷¹, F. Lacava^{70a,70b}, J. Lacey⁴⁴, D.P.J. Lack⁹⁸, H. Lacker¹⁹, D. Lacour¹³³, E. Ladygin⁷⁷, R. Lafaye⁵, B. Laforge¹³³, T. Lagouri^{32c}, S. Lai⁵¹, S. Lammers⁶³, W. Lampl⁷, E. Lançon²⁹, U. Landgraf⁵⁰, M.P.J. Landon⁹⁰, M.C. Lanfermann⁵², V.S. Lang⁴⁴, J.C. Lange¹⁴, R.J. Langenberg³⁵, A.J. Lankford¹⁶⁸, F. Lanni²⁹, K. Lantzsch²⁴, A. Lanza^{68a}, A. Lapertosa^{53b,53a}, S. Laplace¹³³, J.F. Laporte¹⁴², T. Lari^{66a}, F. Lasagni Manghi^{23b,23a}, M. Lassnig³⁵, T.S. Lau^{61a}, A. Laudrain¹²⁹, M. Lavorgna^{67a,67b}, A.T. Law¹⁴³, P. Laycock⁸⁸, M. Lazzaroni^{66a,66b}, B. Le¹⁰², O. Le Dortz¹³³, E. Le Guirriec⁹⁹, E.P. Le Quilleuc¹⁴², M. LeBlanc⁷, T. LeCompte⁶, F. Ledroit-Guillon⁵⁶, C.A. Lee²⁹, G.R. Lee^{144a}, L. Lee⁵⁷, S.C. Lee¹⁵⁵, B. Lefebvre¹⁰¹, M. Lefebvre¹⁷³, F. Legger¹¹², C. Leggett¹⁸, N. Lehmann¹⁷⁹, G. Lehmann Miotto³⁵, W.A. Leight⁴⁴, A. Leisos^{159,w}, M.A.L. Leite^{78d}, R. Leitner¹⁴⁰, D. Lellouch¹⁷⁷, B. Lemmer⁵¹, K.J.C. Leney⁹², T. Lenz²⁴, B. Lenzi³⁵, R. Leone⁷, S. Leone^{69a}, C. Leonidopoulos⁴⁸, G. Lerner¹⁵³, C. Leroy¹⁰⁷, R. Les¹⁶⁴, A.A.J. Lesage¹⁴², C.G. Lester³¹, M. Levchenko¹³⁵, J. Levêque⁵, D. Levin¹⁰³, L.J. Levinson¹⁷⁷, D. Lewis⁹⁰, B. Li¹⁰³, C.-Q. Li^{58a,ak}, H. Li^{58b}, L. Li^{58c}, Q. Li^{15d}, Q.Y. Li^{58a}, S. Li^{58d,58c}, X. Li^{58c}, Y. Li¹⁴⁸, Z. Liang^{15a}, B. Liberti^{71a}, A. Liblong¹⁶⁴, K. Lie^{61c}, S. Liem¹¹⁸, A. Limosani¹⁵⁴, C.Y. Lin³¹, K. Lin¹⁰⁴, T.H. Lin⁹⁷, R.A. Linck⁶³, B.E. Lindquist¹⁵², A.L. Lioni⁵², E. Lipeles¹³⁴, A. Lipniacka¹⁷, M. Lisovsky^{59b}, T.M. Liss^{170,ar}, A. Lister¹⁷², A.M. Litke¹⁴³, J.D. Little⁸, B. Liu⁷⁶, B.L. Liu⁶, H.B. Liu²⁹, H. Liu¹⁰³, J.B. Liu^{58a}, J.K.K. Liu¹³², K. Liu¹³³, M. Liu^{58a}, P. Liu¹⁸, Y. Liu^{15a}, Y.L. Liu^{58a}, Y.W. Liu^{58a}, M. Livan^{68a,68b}, A. Lleres⁵⁶, J. Llorente Merino^{15a}, S.L. Lloyd⁹⁰, C.Y. Lo^{61b}, F. Lo Sterzo⁴¹, E.M. Lobodzinska⁴⁴, P. Loch⁷, K.M. Loew²⁶, T. Lohse¹⁹, K. Lohwasser¹⁴⁶, M. Lokajicek¹³⁸, B.A. Long²⁵, J.D. Long¹⁷⁰, R.E. Long⁸⁷, L. Longo^{65a,65b}, K.A. Looper¹²³, J.A. Lopez^{144b}, I. Lopez Paz¹⁴, A. Lopez Solis¹⁴⁶, J. Lorenz¹¹², N. Lorenzo Martinez⁵, M. Losada²², P.J. Lösel¹¹², A. Lösle⁵⁰, X. Lou⁴⁴, X. Lou^{15a}, A. Lounis¹²⁹, J. Love⁶, P.A. Love⁸⁷, J.J. Lozano Bahilo¹⁷¹, H. Lu^{61a}, M. Lu^{58a}, N. Lu¹⁰³, Y.J. Lu⁶², H.J. Lubatti¹⁴⁵, C. Luci^{70a,70b}, A. Lucotte⁵⁶, C. Luedtke⁵⁰, F. Luehring⁶³, I. Luise¹³³, W. Lukas⁷⁴, L. Luminari^{70a}, B. Lund-Jensen¹⁵¹, M.S. Lutz¹⁰⁰, P.M. Luzi¹³³, D. Lynn²⁹, R. Lysak¹³⁸, E. Lytken⁹⁴, F. Lyu^{15a}, V. Lyubushkin⁷⁷, H. Ma²⁹, L.L. Ma^{58b}, Y. Ma^{58b}, G. Maccarrone⁴⁹, A. Macchiolo¹¹³, C.M. Macdonald¹⁴⁶, J. Machado Miguens^{134,137b}, D. Madaffari¹⁷¹, R. Madar³⁷, W.F. Mader⁴⁶, A. Madsen⁴⁴, N. Madysa⁴⁶, J. Maeda⁸⁰, K. Maekawa¹⁶⁰, S. Maeland¹⁷, T. Maeno²⁹, A.S. Maevskiy¹¹¹, V. Magerl⁵⁰, C. Maidantchik^{78b}, T. Maier¹¹², A. Maio^{137a,137b,137d}, O. Majersky^{28a}, S. Majewski¹²⁸, Y. Makida⁷⁹, N. Makovec¹²⁹, B. Malaescu¹³³, Pa. Malecki⁸², V.P. Maleev¹³⁵, F. Malek⁵⁶, U. Mallik⁷⁵, D. Malon⁶, C. Malone³¹, S. Maltezos¹⁰, S. Malyukov³⁵, J. Mamuzic¹⁷¹, G. Mancini⁴⁹, I. Mandić⁸⁹, J. Maneira^{137a}, L. Manhaes de Andrade Filho^{78a}, J. Manjarres Ramos⁴⁶, K.H. Mankinen⁹⁴, A. Mann¹¹², A. Manousos⁷⁴, B. Mansoulie¹⁴², J.D. Mansour^{15a}, M. Mantoani⁵¹, S. Manzoni^{66a,66b}, G. Marceca³⁰, L. March⁵², L. Marchese¹³², G. Marchiori¹³³, M. Marcisovsky¹³⁸, C.A. Marin Tobon³⁵, M. Marjanovic³⁷, D.E. Marley¹⁰³, F. Marroquim^{78b}, Z. Marshall¹⁸, M.U.F. Martensson¹⁶⁹, S. Marti-Garcia¹⁷¹, C.B. Martin¹²³, T.A. Martin¹⁷⁵, V.J. Martin⁴⁸, B. Martin dit Latour¹⁷, M. Martinez^{14,z}, V.I. Martinez Outschoorn¹⁰⁰, S. Martin-Haugh¹⁴¹, V.S. Martoiu^{27b}, A.C. Martyniuk⁹², A. Marzin³⁵, L. Masetti⁹⁷, T. Mashimo¹⁶⁰, R. Mashinistov¹⁰⁸, J. Masik⁹⁸, A.L. Maslennikov^{120b,120a}, L.H. Mason¹⁰², L. Massa^{71a,71b}, P. Mastrandrea⁵, A. Mastroberardino^{40b,40a}, T. Masubuchi¹⁶⁰, P. Mättig¹⁷⁹, J. Maurer^{27b}

B. Maček⁸⁹, S.J. Maxfield⁸⁸, D.A. Maximov^{120b,120a}, R. Mazini¹⁵⁵, I. Maznas¹⁵⁹, S.M. Mazza¹⁴³, N.C. Mc Fadden¹¹⁶, G. Mc Goldrick¹⁶⁴, S.P. Mc Kee¹⁰³, A. McCarn¹⁰³, T.G. McCarthy¹¹³, L.I. McClymont⁹², E.F. McDonald¹⁰², J.A. Mcfayden³⁵, G. Mchedlidze⁵¹, M.A. McKay⁴¹, K.D. McLean¹⁷³, S.J. McMahan¹⁴¹, P.C. McNamara¹⁰², C.J. McNicol¹⁷⁵, R.A. McPherson^{173,ad}, J.E. Mdhluli^{32c}, Z.A. Meadows¹⁰⁰, S. Meehan¹⁴⁵, T.M. Megy⁵⁰, S. Mehlhase¹¹², A. Mehta⁸⁸, T. Meideck⁵⁶, B. Meirose⁴², D. Melini^{171,h}, B.R. Mellado Garcia^{32c}, J.D. Mellenthin⁵¹, M. Melo^{28a}, F. Meloni⁴⁴, A. Melzer²⁴, S.B. Menary⁹⁸, E.D. Mendes Gouveia^{137a}, L. Meng⁸⁸, X.T. Meng¹⁰³, A. Mengarelli^{23b,23a}, S. Menke¹¹³, E. Meoni^{40b,40a}, S. Mergelmeyer¹⁹, C. Merlassino²⁰, P. Mermod⁵², L. Merola^{67a,67b}, C. Meroni^{66a}, F.S. Merritt³⁶, A. Messina^{70a,70b}, J. Metcalfe⁶, A.S. Mete¹⁶⁸, C. Meyer¹³⁴, J. Meyer¹⁵⁷, J.-P. Meyer¹⁴², H. Meyer Zu Theenhausen^{59a}, F. Miano¹⁵³, R.P. Middleton¹⁴¹, L. Mijović⁴⁸, G. Mikenberg¹⁷⁷, M. Mikestikova¹³⁸, M. Mikuz⁸⁹, M. Milesi¹⁰², A. Milic¹⁶⁴, D.A. Millar⁹⁰, D.W. Miller³⁶, A. Milov¹⁷⁷, D.A. Milstead^{43a,43b}, A.A. Minaenko¹²¹, M. Miñano Moya¹⁷¹, I.A. Minashvili^{156b}, A.I. Mincer¹²², B. Mindur^{81a}, M. Mineev⁷⁷, Y. Minegishi¹⁶⁰, Y. Ming¹⁷⁸, L.M. Mir¹⁴, A. Mirto^{65a,65b}, K.P. Mistry¹³⁴, T. Mitani¹⁷⁶, J. Mitrevski¹¹², V.A. Mitsou¹⁷¹, A. Miucci²⁰, P.S. Miyagawa¹⁴⁶, A. Mizukami⁷⁹, J.U. Mjörnmark⁹⁴, T. Mkrtchyan¹⁸¹, M. Mlynarikova¹⁴⁰, T. Moa^{43a,43b}, K. Mochizuki¹⁰⁷, P. Mogg⁵⁰, S. Mohapatra³⁸, S. Molander^{43a,43b}, R. Moles-Valls²⁴, M.C. Mondragon¹⁰⁴, K. Mönig⁴⁴, J. Monk³⁹, E. Monnier⁹⁹, A. Montalbano¹⁴⁹, J. Montejo Berlingen³⁵, F. Monticelli⁸⁶, S. Monzani^{66a}, R.W. Moore³, N. Morange¹²⁹, D. Moreno²², M. Moreno Llácer³⁵, P. Morettini^{53b}, M. Morgenstern¹¹⁸, S. Morgenstern⁴⁶, D. Mori¹⁴⁹, T. Mori¹⁶⁰, M. Morii⁵⁷, M. Morinaga¹⁷⁶, V. Morisbak¹³¹, A.K. Morley³⁵, G. Mornacchi³⁵, A.P. Morris⁹², J.D. Morris⁹⁰, L. Morvaj¹⁵², P. Moschovakos¹⁰, M. Mosidze^{156b}, H.J. Moss¹⁴⁶, J. Moss^{150,n}, K. Motohashi¹⁶², R. Mount¹⁵⁰, E. Mountricha³⁵, E.J.W. Moyse¹⁰⁰, S. Muanza⁹⁹, F. Mueller¹¹³, J. Mueller¹³⁶, R.S.P. Mueller¹¹², D. Muenstermann⁸⁷, P. Mullen⁵⁵, G.A. Mullier²⁰, F.J. Munoz Sanchez⁹⁸, P. Murin^{28b}, W.J. Murray^{175,141}, A. Murrone^{66a,66b}, M. Muškinja⁸⁹, C. Mwewa^{32a}, A.G. Myagkov^{121,am}, J. Myers¹²⁸, M. Myska¹³⁹, B.P. Nachman¹⁸, O. Nackenhorst⁴⁵, K. Nagai¹³², K. Nagano⁷⁹, Y. Nagasaka⁶⁰, K. Nagata¹⁶⁶, M. Nagel⁵⁰, E. Nagy⁹⁹, A.M. Nairz³⁵, Y. Nakahama¹¹⁵, K. Nakamura⁷⁹, T. Nakamura¹⁶⁰, I. Nakano¹²⁴, H. Nanjo¹³⁰, F. Napolitano^{59a}, R.F. Naranjo Garcia⁴⁴, R. Narayan¹¹, D.I. Narrias Villar^{59a}, I. Naryshkin¹³⁵, T. Naumann⁴⁴, G. Navarro²², R. Nayyar⁷, H.A. Neal^{103,*}, P.Y. Nechaeva¹⁰⁸, T.J. Neep¹⁴², A. Negri^{68a,68b}, M. Negrini^{23b}, S. Nektarijevic¹¹⁷, C. Nellist⁵¹, M.E. Nelson¹³², S. Nemecek¹³⁸, P. Nemethy¹²², M. Nessi^{35,f}, M.S. Neubauer¹⁷⁰, M. Neumann¹⁷⁹, P.R. Newman²¹, T.Y. Ng^{61c}, Y.S. Ng¹⁹, H.D.N. Nguyen⁹⁹, T. Nguyen Manh¹⁰⁷, E. Nibigira³⁷, R.B. Nickerson¹³², R. Nicolaidou¹⁴², J. Nielsen¹⁴³, N. Nikiforou¹¹, V. Nikolaenko^{121,am}, I. Nikolic-Audit¹³³, K. Nikolopoulos²¹, P. Nilsson²⁹, Y. Ninomiya⁷⁹, A. Nisati^{70a}, N. Nishu^{58c}, R. Nisius¹¹³, I. Nitsche⁴⁵, T. Nitta¹⁷⁶, T. Nobe¹⁶⁰, Y. Noguchi⁸³, M. Nomachi¹³⁰, I. Nomidis¹³³, M.A. Nomura²⁹, T. Nooney⁹⁰, M. Nordberg³⁵, N. Norjoharuddeen¹³², T. Novak⁸⁹, O. Novgorodova⁴⁶, R. Novotny¹³⁹, L. Nozka¹²⁷, K. Ntekas¹⁶⁸, E. Nurse⁹², F. Nuti¹⁰², F.G. Oakham^{33,au}, H. Oberlack¹¹³, T. Obermann²⁴, J. Ocariz¹³³, A. Ochi⁸⁰, I. Ochoa³⁸, J.P. Ochoa-Ricoux^{144a}, K. O'Connor²⁶, S. Oda⁸⁵, S. Odaka⁷⁹, S. Oerdek⁵¹, A. Oh⁹⁸, S.H. Oh⁴⁷, C.C. Ohm¹⁵¹, H. Oide^{53b,53a}, H. Okawa¹⁶⁶, Y. Okazaki⁸³, Y. Okumura¹⁶⁰, T. Okuyama⁷⁹, A. Olariu^{27b}, L.F. Oleiro Seabra^{137a}, S.A. Olivares Pino^{144a}, D. Oliveira Damazio²⁹, J.L. Oliver¹, M.J.R. Olsson³⁶, A. Olszewski⁸², J. Olszowska⁸², D.C. O'Neil¹⁴⁹, A. Onofre^{137a,137e}, K. Onogi¹¹⁵, P.U.E. Onyisi¹¹, H. Oppen¹³¹, M.J. Oreglia³⁶, Y. Oren¹⁵⁸, D. Orestano^{72a,72b}, E.C. Orgill⁹⁸, N. Orlando^{61b}, A.A. O'Rourke⁴⁴, R.S. Orr¹⁶⁴, B. Osculati^{53b,53a,*}, V. O'Shea⁵⁵, R. Ospanov^{58a}, G. Otero y Garzon³⁰, H. Otono⁸⁵, M. Ouchrif^{34d}, F. Ould-Saada¹³¹, A. Ouraou¹⁴², Q. Ouyang^{15a}, M. Owen⁵⁵, R.E. Owen²¹, V.E. Ozcan^{12c}, N. Ozturk⁸, J. Pacalt¹²⁷, H.A. Pacey³¹, K. Pachal¹⁴⁹, A. Pacheco Pages¹⁴, L. Pacheco Rodriguez¹⁴², C. Padilla Aranda¹⁴, S. Pagan Griso¹⁸, M. Paganini¹⁸⁰, G. Palacino⁶³, S. Palazzo^{40b,40a}, S. Palestini³⁵, M. Palka^{81b}, D. Pallin³⁷, I. Panagoulas¹⁰, C.E. Pandini³⁵, J.G. Panduro Vazquez⁹¹, P. Pani³⁵, G. Panizzo^{64a,64c}, L. Paolozzi⁵², T.D. Papadopoulou¹⁰, K. Papageorgiou^{9,j}, A. Paramonov⁶, D. Paredes Hernandez^{61b}, S.R. Paredes Saenz¹³², B. Parida^{58c}, A.J. Parker⁸⁷, K.A. Parker⁴⁴, M.A. Parker³¹, F. Parodi^{53b,53a}, J.A. Parsons³⁸, U. Parzefall⁵⁰, V.R. Pascuzzi¹⁶⁴, J.M.P. Pasner¹⁴³, E. Pasqualucci^{70a}, S. Passaggio^{53b}, F. Pastore⁹¹, P. Pasuwan^{43a,43b}, S. Pataria⁹⁷, J.R. Pater⁹⁸, A. Pathak^{178,k}, T. Pauly³⁵, B. Pearson¹¹³, M. Pedersen¹³¹, L. Pedraza Diaz¹¹⁷, R. Pedro^{137a,137b}, S.V. Peleganchuk^{120b,120a}, O. Penc¹³⁸, C. Peng^{15d}, H. Peng^{58a}, B.S. Peralva^{78a}, M.M. Perego¹⁴², A.P. Pereira Peixoto^{137a}, D.V. Perepelitsa²⁹, F. Peri¹⁹, L. Perini^{66a,66b}, H. Pernegger³⁵, S. Perrella^{67a,67b}, V.D. Peshekhonov^{77,*}, K. Peters⁴⁴, R.F.Y. Peters⁹⁸,

B.A. Petersen³⁵, T.C. Petersen³⁹, E. Petit⁵⁶, A. Petridis¹, C. Petridou¹⁵⁹, P. Petroff¹²⁹, E. Petrolo^{70a}, M. Petrov¹³², F. Petrucci^{72a,72b}, M. Pettee¹⁸⁰, N.E. Pettersson¹⁰⁰, A. Peyaud¹⁴², R. Pezoa^{144b}, T. Pham¹⁰², F.H. Phillips¹⁰⁴, P.W. Phillips¹⁴¹, G. Piacquadio¹⁵², E. Pianori¹⁸, A. Picazio¹⁰⁰, M.A. Pickering¹³², R. Piegai³⁰, J.E. Pilcher³⁶, A.D. Pilkington⁹⁸, M. Pinamonti^{71a,71b}, J.L. Pinfold³, M. Pitt¹⁷⁷, M.-A. Pleier²⁹, V. Pleskot¹⁴⁰, E. Plotnikova⁷⁷, D. Pluth⁷⁶, P. Podberezko^{120b,120a}, R. Poettgen⁹⁴, R. Poggi⁵², L. Poggioli¹²⁹, I. Pogrebnyak¹⁰⁴, D. Pohl²⁴, I. Pokharel⁵¹, G. Polesello^{68a}, A. Poley⁴⁴, A. Policicchio^{40b,40a}, R. Polifka³⁵, A. Polini^{23b}, C.S. Pollard⁴⁴, V. Polychronakos²⁹, D. Ponomarenko¹¹⁰, L. Pontecorvo³⁵, G.A. Popeneciu^{27d}, D.M. Portillo Quintero¹³³, S. Pospisil¹³⁹, K. Potamianos⁴⁴, I.N. Potrap⁷⁷, C.J. Potter³¹, H. Potti¹¹, T. Poulsen⁹⁴, J. Poveda³⁵, T.D. Powell¹⁴⁶, M.E. Pozo Astigarraga³⁵, P. Pralavorio⁹⁹, S. Prell⁷⁶, D. Price⁹⁸, M. Primavera^{65a}, S. Prince¹⁰¹, N. Proklova¹¹⁰, K. Prokofiev^{61c}, F. Prokoshin^{144b}, S. Protopopescu²⁹, J. Proudfoot⁶, M. Przybycien^{81a}, A. Puri¹⁷⁰, P. Puzo¹²⁹, J. Qian¹⁰³, Y. Qin⁹⁸, A. Quadt⁵¹, M. Queitsch-Maitland⁴⁴, A. Qureshi¹, P. Rados¹⁰², F. Ragusa^{66a,66b}, G. Rahal⁹⁵, J.A. Raine⁹⁸, S. Rajagopalan²⁹, A. Ramirez Morales⁹⁰, T. Rashid¹²⁹, S. Raspopov⁵, M.G. Ratti^{66a,66b}, D.M. Rauch⁴⁴, F. Rauscher¹¹², S. Rave⁹⁷, B. Ravina¹⁴⁶, I. Ravinovich¹⁷⁷, J.H. Rawling⁹⁸, M. Raymond³⁵, A.L. Read¹³¹, N.P. Readioff⁵⁶, M. Reale^{65a,65b}, D.M. Rebuzzi^{68a,68b}, A. Redelbach¹⁷⁴, G. Redlinger²⁹, R. Reece¹⁴³, R.G. Reed^{32c}, K. Reeves⁴², L. Rehnisch¹⁹, J. Reichert¹³⁴, A. Reiss⁹⁷, C. Rembser³⁵, H. Ren^{15d}, M. Rescigno^{70a}, S. Resconi^{66a}, E.D. Resseguie¹³⁴, S. Rettie¹⁷², E. Reynolds²¹, O.L. Rezanova^{120b,120a}, P. Reznicek¹⁴⁰, R. Richter¹¹³, S. Richter⁹², E. Richter-Was^{81b}, O. Ricken²⁴, M. Ridel¹³³, P. Rieck¹¹³, C.J. Riegel¹⁷⁹, O. Rifki⁴⁴, M. Rijssenbeek¹⁵², A. Rimoldi^{68a,68b}, M. Rimoldi²⁰, L. Rinaldi^{23b}, G. Ripellino¹⁵¹, B. Ristić⁸⁷, E. Ritsch³⁵, I. Riu¹⁴, J.C. Rivera Vergara^{144a}, F. Rizatdinova¹²⁶, E. Rizvi⁹⁰, C. Rizzi¹⁴, R.T. Roberts⁹⁸, S.H. Robertson^{101,ad}, A. Robichaud-Veronneau¹⁰¹, D. Robinson³¹, J.E.M. Robinson⁴⁴, A. Robson⁵⁵, E. Rocco⁹⁷, C. Roda^{69a,69b}, Y. Rodina⁹⁹, S. Rodriguez Bosca¹⁷¹, A. Rodriguez Perez¹⁴, D. Rodriguez Rodriguez¹⁷¹, A.M. Rodríguez Vera^{165b}, S. Roe³⁵, C.S. Rogan⁵⁷, O. Røhne¹³¹, R. Røhrig¹¹³, C.P.A. Roland⁶³, J. Roloff⁵⁷, A. Romaniouk¹¹⁰, M. Romano^{23b,23a}, N. Rompotis⁸⁸, M. Ronzani¹²², L. Roos¹³³, S. Rosati^{70a}, K. Rosbach⁵⁰, P. Rose¹⁴³, N.-A. Rosien⁵¹, E. Rossi^{67a,67b}, L.P. Rossi^{53b}, L. Rossini^{66a,66b}, J.H.N. Rosten³¹, R. Rosten¹⁴, M. Rotaru^{27b}, J. Rothberg¹⁴⁵, D. Rousseau¹²⁹, D. Roy^{32c}, A. Rozanov⁹⁹, Y. Rozen¹⁵⁷, X. Ruan^{32c}, F. Rubbo¹⁵⁰, F. Rühr⁵⁰, A. Ruiz-Martinez¹⁷¹, Z. Rurikova⁵⁰, N.A. Rusakovich⁷⁷, H.L. Russell¹⁰¹, J.P. Rutherford⁷, E.M. Rüttinger^{44,l}, Y.F. Ryabov¹³⁵, M. Rybar¹⁷⁰, G. Rybkin¹²⁹, S. Ryu⁶, A. Ryzhov¹²¹, G.F. Rzehorz⁵¹, P. Sabatini⁵¹, G. Sabato¹¹⁸, S. Sacerdoti¹²⁹, H.F.-W. Sadrozinski¹⁴³, R. Sadykov⁷⁷, F. Safai Tehrani^{70a}, P. Saha¹¹⁹, M. Sahinsoy^{59a}, A. Sahu¹⁷⁹, M. Saimpert⁴⁴, M. Saito¹⁶⁰, T. Saito¹⁶⁰, H. Sakamoto¹⁶⁰, A. Sakharov^{122,al}, D. Salamani⁵², G. Salamanna^{72a,72b}, J.E. Salazar Loyola^{144b}, D. Salek¹¹⁸, P.H. Sales De Bruin¹⁶⁹, D. Salihagic¹¹³, A. Salnikov¹⁵⁰, J. Salt¹⁷¹, D. Salvatore^{40b,40a}, F. Salvatore¹⁵³, A. Salvucci^{61a,61b,61c}, A. Salzburger³⁵, J. Samarati³⁵, D. Sammel⁵⁰, D. Sampsonidis¹⁵⁹, D. Sampsonidou¹⁵⁹, J. Sánchez¹⁷¹, A. Sanchez Pineda^{64a,64c}, H. Sandaker¹³¹, C.O. Sander⁴⁴, M. Sandhoff¹⁷⁹, C. Sandoval²², D.P.C. Sankey¹⁴¹, M. Sannino^{53b,53a}, Y. Sano¹¹⁵, A. Sansoni⁴⁹, C. Santoni³⁷, H. Santos^{137a}, I. Santoyo Castillo¹⁵³, A. Saponov⁷⁷, J.G. Saraiva^{137a,137d}, O. Sasaki⁷⁹, K. Sato¹⁶⁶, E. Sauvan⁵, P. Savard^{164,au}, N. Savic¹¹³, R. Sawada¹⁶⁰, C. Sawyer¹⁴¹, L. Sawyer^{93,aj}, C. Sbarra^{23b}, A. Sbrizzi^{23b,23a}, T. Scanlon⁹², J. Schaarschmidt¹⁴⁵, P. Schacht¹¹³, B.M. Schachtner¹¹², D. Schaefer³⁶, L. Schaefer¹³⁴, J. Schaeffer⁹⁷, S. Schaepe³⁵, U. Schäfer⁹⁷, A.C. Schaffer¹²⁹, D. Schaile¹¹², R.D. Schamberger¹⁵², N. Scharmberg⁹⁸, V.A. Schegelsky¹³⁵, D. Scheirich¹⁴⁰, F. Schenck¹⁹, M. Schernau¹⁶⁸, C. Schiavi^{53b,53a}, S. Schier¹⁴³, L.K. Schildgen²⁴, Z.M. Schillaci²⁶, E.J. Schioppa³⁵, M. Schioppa^{40b,40a}, K.E. Schleicher⁵⁰, S. Schlenker³⁵, K.R. Schmidt-Sommerfeld¹¹³, K. Schmieden³⁵, C. Schmitt⁹⁷, S. Schmitt⁴⁴, S. Schmitz⁹⁷, U. Schnoor⁵⁰, L. Schoeffel¹⁴², A. Schoening^{59b}, E. Schopf²⁴, M. Schott⁹⁷, J.F.P. Schouwenberg¹¹⁷, J. Schovancova³⁵, S. Schramm⁵², A. Schulte⁹⁷, H.-C. Schultz-Coulon^{59a}, M. Schumacher⁵⁰, B.A. Schumm¹⁴³, Ph. Schune¹⁴², A. Schwartzman¹⁵⁰, T.A. Schwarz¹⁰³, H. Schweiger⁹⁸, Ph. Schwemling¹⁴², R. Schwienhorst¹⁰⁴, A. Sciandra²⁴, G. Sciolla²⁶, M. Scornajenghi^{40b,40a}, F. Scuri^{69a}, F. Scutti¹⁰², L.M. Scyboz¹¹³, J. Searcy¹⁰³, C.D. Sebastiani^{70a,70b}, P. Seema²⁴, S.C. Seidel¹¹⁶, A. Seiden¹⁴³, T. Seiss³⁶, J.M. Seixas^{78b}, G. Sekhniaidze^{67a}, K. Sekhon¹⁰³, S.J. Sekula⁴¹, N. Semprini-Cesari^{23b,23a}, S. Sen⁴⁷, S. Senkin³⁷, C. Serfon¹³¹, L. Serin¹²⁹, L. Serkin^{64a,64b}, M. Sessa^{72a,72b}, H. Severini¹²⁵, F. Sforza¹⁶⁷, A. Sfyrly⁵², E. Shabalina⁵¹, J.D. Shahinian¹⁴³, N.W. Shaikh^{43a,43b}, L.Y. Shan^{15a}, R. Shang¹⁷⁰, J.T. Shank²⁵, M. Shapiro¹⁸, A.S. Sharma¹, A. Sharma¹³², P.B. Shatalov¹⁰⁹, K. Shaw¹⁵³, S.M. Shaw⁹⁸, A. Shcherbakova¹³⁵, Y. Shen¹²⁵, N. Sherafati³³,

A.D. Sherman²⁵, P. Sherwood⁹², L. Shi^{155,aq}, S. Shimizu⁸⁰, C.O. Shimmin¹⁸⁰, M. Shimojima¹¹⁴, I.P.J. Shipsey¹³², S. Shirabe⁸⁵, M. Shiyakova⁷⁷, J. Shlomi¹⁷⁷, A. Shmeleva¹⁰⁸, D. Shoaleh Saadi¹⁰⁷, M.J. Shochet³⁶, S. Shojaii¹⁰², D.R. Shope¹²⁵, S. Shrestha¹²³, E. Shulga¹¹⁰, P. Sicho¹³⁸, A.M. Sickles¹⁷⁰, P.E. Sidebo¹⁵¹, E. Sideras Haddad^{32c}, O. Sidiropoulou¹⁷⁴, A. Sidoti^{23b,23a}, F. Siegert⁴⁶, Dj. Sijacki¹⁶, J. Silva^{137a}, M. Silva Jr.¹⁷⁸, M.V. Silva Oliveira^{78a}, S.B. Silverstein^{43a}, L. Simic⁷⁷, S. Simion¹²⁹, E. Simioni⁹⁷, M. Simon⁹⁷, R. Simoniello⁹⁷, P. Sinervo¹⁶⁴, N.B. Sinev¹²⁸, M. Sioli^{23b,23a}, G. Siragusa¹⁷⁴, I. Siral¹⁰³, S.Yu. Sivoklokov¹¹¹, J. Sjölin^{43a,43b}, M.B. Skinner⁸⁷, P. Skubic¹²⁵, M. Slater²¹, T. Slavicek¹³⁹, M. Slawinska⁸², K. Sliwa¹⁶⁷, R. Slovak¹⁴⁰, V. Smakhtin¹⁷⁷, B.H. Smart⁵, J. Smiesko^{28a}, N. Smirnov¹¹⁰, S.Yu. Smirnov¹¹⁰, Y. Smirnov¹¹⁰, L.N. Smirnova¹¹¹, O. Smirnova⁹⁴, J.W. Smith⁵¹, M.N.K. Smith³⁸, R.W. Smith³⁸, M. Smizanska⁸⁷, K. Smolek¹³⁹, A.A. Snesarev¹⁰⁸, I.M. Snyder¹²⁸, S. Snyder²⁹, R. Sobie^{173,ad}, A.M. Soffa¹⁶⁸, A. Soffer¹⁵⁸, A. Søgaard⁴⁸, D.A. Soh¹⁵⁵, G. Sokhrannyi⁸⁹, C.A. Solans Sanchez³⁵, M. Solar¹³⁹, E.Yu. Soldatov¹¹⁰, U. Soldevila¹⁷¹, A.A. Solodkov¹²¹, A. Soloshenko⁷⁷, O.V. Solovyanov¹²¹, V. Solovyev¹³⁵, P. Sommer¹⁴⁶, H. Son¹⁶⁷, W. Song¹⁴¹, A. Sopczak¹³⁹, F. Sopkova^{28b}, D. Sosa^{59b}, C.L. Sotiropoulou^{69a,69b}, S. Sottocornola^{68a,68b}, R. Soualah^{64a,64c,i}, A.M. Soukharev^{120b,120a}, D. South⁴⁴, B.C. Sowden⁹¹, S. Spagnolo^{65a,65b}, M. Spalla¹¹³, M. Spangenberg¹⁷⁵, F. Spanò⁹¹, D. Sperlich¹⁹, F. Spettel¹¹³, T.M. Spieker^{59a}, R. Spighi^{23b}, G. Spigo³⁵, L.A. Spiller¹⁰², D.P. Spiteri⁵⁵, M. Spousta¹⁴⁰, A. Stabile^{66a,66b}, R. Stamen^{59a}, S. Stamm¹⁹, E. Stanecka⁸², R.W. Stanek⁶, C. Stanescu^{72a}, B. Stanislaus¹³², M.M. Stanitzki⁴⁴, B. Stapf¹¹⁸, S. Stapnes¹³¹, E.A. Starchenko¹²¹, G.H. Stark³⁶, J. Stark⁵⁶, S.H. Stark³⁹, P. Staroba¹³⁸, P. Starovoitov^{59a}, S. Stärz³⁵, R. Staszewski⁸², M. Stegler⁴⁴, P. Steinberg²⁹, B. Stelzer¹⁴⁹, H.J. Stelzer³⁵, O. Stelzer-Chilton^{165a}, H. Stenzel⁵⁴, T.J. Stevenson⁹⁰, G.A. Stewart⁵⁵, M.C. Stockton¹²⁸, G. Stoica^{27b}, P. Stolte⁵¹, S. Stonjek¹¹³, A. Straessner⁴⁶, J. Strandberg¹⁵¹, S. Strandberg^{43a,43b}, M. Strauss¹²⁵, P. Strizenec^{28b}, R. Ströhmer¹⁷⁴, D.M. Strom¹²⁸, R. Stroynowski⁴¹, A. Strubig⁴⁸, S.A. Stucci²⁹, B. Stugu¹⁷, J. Stupak¹²⁵, N.A. Styles⁴⁴, D. Su¹⁵⁰, J. Su¹³⁶, S. Suchek^{59a}, Y. Sugaya¹³⁰, M. Suk¹³⁹, V.V. Sulin¹⁰⁸, D.M.S. Sultan⁵², S. Sultansoy^{4c}, T. Sumida⁸³, S. Sun¹⁰³, X. Sun³, K. Suruliz¹⁵³, C.J.E. Suster¹⁵⁴, M.R. Sutton¹⁵³, S. Suzuki⁷⁹, M. Svatos¹³⁸, M. Swiatlowski³⁶, S.P. Swift², A. Sydorenko⁹⁷, I. Sykora^{28a}, T. Sykora¹⁴⁰, D. Ta⁹⁷, K. Tackmann^{44,aa}, J. Taenzer¹⁵⁸, A. Taffard¹⁶⁸, R. Tafirout^{165a}, E. Tahirovic⁹⁰, N. Taiblum¹⁵⁸, H. Takai²⁹, R. Takashima⁸⁴, E.H. Takasugi¹¹³, K. Takeda⁸⁰, T. Takeshita¹⁴⁷, Y. Takubo⁷⁹, M. Talby⁹⁹, A.A. Talyshev^{120b,120a}, J. Tanaka¹⁶⁰, M. Tanaka¹⁶², R. Tanaka¹²⁹, R. Tanioka⁸⁰, B.B. Tannenwald¹²³, S. Tapia Araya^{144b}, S. Tapprogge⁹⁷, A. Tarek Abouelfadl Mohamed¹³³, S. Tarem¹⁵⁷, G. Tarna^{27b,e}, G.F. Tartarelli^{66a}, P. Tas¹⁴⁰, M. Tasevsky¹³⁸, T. Tashiro⁸³, E. Tassi^{40b,40a}, A. Tavares Delgado^{137a,137b}, Y. Tayalati^{34e}, A.C. Taylor¹¹⁶, A.J. Taylor⁴⁸, G.N. Taylor¹⁰², P.T.E. Taylor¹⁰², W. Taylor^{165b}, A.S. Tee⁸⁷, P. Teixeira-Dias⁹¹, H. Ten Kate³⁵, P.K. Teng¹⁵⁵, J.J. Teoh¹¹⁸, F. Tepel¹⁷⁹, S. Terada⁷⁹, K. Terashi¹⁶⁰, J. Terron⁹⁶, S. Terzo¹⁴, M. Testa⁴⁹, R.J. Teuscher^{164,ad}, S.J. Thais¹⁸⁰, T. Theveneaux-Pelzer⁴⁴, F. Thiele³⁹, J.P. Thomas²¹, A.S. Thompson⁵⁵, P.D. Thompson²¹, L.A. Thomsen¹⁸⁰, E. Thomson¹³⁴, Y. Tian³⁸, R.E. Ticse Torres⁵¹, V.O. Tikhomirov^{108,an}, Yu.A. Tikhonov^{120b,120a}, S. Timoshenko¹¹⁰, P. Tipton¹⁸⁰, S. Tisserant⁹⁹, K. Todome¹⁶², S. Todorova-Nova⁵, S. Todt⁴⁶, J. Tojo⁸⁵, S. Tokár^{28a}, K. Tokushuku⁷⁹, E. Tolley¹²³, K.G. Tomiwa^{32c}, M. Tomoto¹¹⁵, L. Tompkins^{150,q}, K. Toms¹¹⁶, B. Tong⁵⁷, P. Tornambe⁵⁰, E. Torrence¹²⁸, H. Torres⁴⁶, E. Torrò Pastor¹⁴⁵, C. Toscirì¹³², J. Toth^{99,ac}, F. Touchard⁹⁹, D.R. Tovey¹⁴⁶, C.J. Treado¹²², T. Trefzger¹⁷⁴, F. Tresoldi¹⁵³, A. Tricoli²⁹, I.M. Trigger^{165a}, S. Trincaz-Duvoid¹³³, M.F. Tripiana¹⁴, W. Trischuk¹⁶⁴, B. Trocmé⁵⁶, A. Trofymov¹²⁹, C. Troncon^{66a}, M. Trovatelli¹⁷³, F. Trovato¹⁵³, L. Truong^{32b}, M. Trzebinski⁸², A. Trzupek⁸², F. Tsai⁴⁴, J.C.-L. Tseng¹³², P.V. Tsiarehka¹⁰⁵, N. Tsirintanis⁹, V. Tsiskaridze¹⁵², E.G. Tskhadadze^{156a}, I.I. Tsukerman¹⁰⁹, V. Tsulaia¹⁸, S. Tsuno⁷⁹, D. Tsybychev¹⁵², Y. Tu^{61b}, A. Tudorache^{27b}, V. Tudorache^{27b}, T.T. Tulbure^{27a}, A.N. Tuna⁵⁷, S. Turchikhin⁷⁷, D. Turgeman¹⁷⁷, I. Turk Cakir^{4b,u}, R. Turra^{66a}, P.M. Tuts³⁸, E. Tzovara⁹⁷, G. Uccielli^{23b,23a}, I. Ueda⁷⁹, M. Ughetto^{43a,43b}, F. Ukegawa¹⁶⁶, G. Unal³⁵, A. Undrus²⁹, G. Unel¹⁶⁸, F.C. Ungaro¹⁰², Y. Unno⁷⁹, K. Uno¹⁶⁰, J. Urban^{28b}, P. Urquijo¹⁰², P. Urrejola⁹⁷, G. Usai⁸, J. Usui⁷⁹, L. Vacavant⁹⁹, V. Vacek¹³⁹, B. Vachon¹⁰¹, K.O.H. Vadla¹³¹, A. Vaidya⁹², C. Valderanis¹¹², E. Valdes Santurio^{43a,43b}, M. Valente⁵², S. Valentini^{23b,23a}, A. Valero¹⁷¹, L. Valéry⁴⁴, R.A. Vallance²¹, A. Vallier⁵, J.A. Valls Ferrer¹⁷¹, T.R. Van Daalen¹⁴, W. Van Den Wollenberg¹¹⁸, H. Van der Graaf¹¹⁸, P. Van Gemmeren⁶, J. Van Nieuwkoop¹⁴⁹, I. Van Vulpen¹¹⁸, M. Vanadia^{71a,71b}, W. Vandelli³⁵, A. Vaniachine¹⁶³, P. Vankov¹¹⁸, R. Vari^{70a}, E.W. Varnes⁷, C. Varni^{53b,53a}, T. Varol⁴¹, D. Varouchas¹²⁹, K.E. Varvell¹⁵⁴, G.A. Vasquez^{144b}, J.G. Vasquez¹⁸⁰, F. Vazeille³⁷, D. Vazquez Furelos¹⁴,

T. Vazquez Schroeder¹⁰¹, J. Veatch⁵¹, V. Vecchio^{72a,72b}, L.M. Veloce¹⁶⁴, F. Veloso^{137a,137c}, S. Veneziano^{70a}, A. Ventura^{65a,65b}, M. Venturi¹⁷³, N. Venturi³⁵, V. Vercesi^{68a}, M. Verducci^{72a,72b}, C.M. Vergel Infante⁷⁶, W. Verkerke¹¹⁸, A.T. Vermeulen¹¹⁸, J.C. Vermeulen¹¹⁸, M.C. Vetterli^{149,au}, N. Viaux Maira^{144b}, M. Vicente Barreto Pinto⁵², I. Vichou^{170,*}, T. Vickey¹⁴⁶, O.E. Vickey Boeriu¹⁴⁶, G.H.A. Viehhauser¹³², S. Viel¹⁸, L. Vigani¹³², M. Villa^{23b,23a}, M. Villaplana Perez^{66a,66b}, E. Vilucchi⁴⁹, M.G. Vincter³³, V.B. Vinogradov⁷⁷, A. Vishwakarma⁴⁴, C. Vittori^{23b,23a}, I. Vivarelli¹⁵³, S. Vlachos¹⁰, M. Vogel¹⁷⁹, P. Vokac¹³⁹, G. Volpi¹⁴, S.E. von Buddenbrock^{32c}, E. Von Toerne²⁴, V. Vorobel¹⁴⁰, K. Vorobev¹¹⁰, M. Vos¹⁷¹, J.H. Vosseveld⁸⁸, N. Vranjes¹⁶, M. Vranjes Milosavljevic¹⁶, V. Vrba¹³⁹, M. Vreeswijk¹¹⁸, T. Šfiligoj⁸⁹, R. Vuillermet³⁵, I. Vukotic³⁶, T. Ženiš^{28a}, L. Živković¹⁶, P. Wagner²⁴, W. Wagner¹⁷⁹, J. Wagner-Kuhr¹¹², H. Wahlberg⁸⁶, S. Wahrmund⁴⁶, K. Wakamiya⁸⁰, V.M. Walbrecht¹¹³, J. Walder⁸⁷, R. Walker¹¹², S.D. Walker⁹¹, W. Walkowiak¹⁴⁸, V. Wallangen^{43a,43b}, A.M. Wang⁵⁷, C. Wang^{58b,e}, F. Wang¹⁷⁸, H. Wang¹⁸, H. Wang³, J. Wang¹⁵⁴, J. Wang^{59b}, P. Wang⁴¹, Q. Wang¹²⁵, R.-J. Wang¹³³, R. Wang^{58a}, R. Wang⁶, S.M. Wang¹⁵⁵, W.T. Wang^{58a}, W. Wang^{15c,ae}, W.X. Wang^{58a,ae}, Y. Wang^{58a,ak}, Z. Wang^{58c}, C. Wanotayaroj⁴⁴, A. Warburton¹⁰¹, C.P. Ward³¹, D.R. Wardrope⁹², A. Washbrook⁴⁸, P.M. Watkins²¹, A.T. Watson²¹, M.F. Watson²¹, G. Watts¹⁴⁵, S. Watts⁹⁸, B.M. Waugh⁹², A.F. Webb¹¹, S. Webb⁹⁷, C. Weber¹⁸⁰, M.S. Weber²⁰, S.A. Weber³³, S.M. Weber^{59a}, J.S. Webster⁶, A.R. Weidberg¹³², B. Weinert⁶³, J. Weingarten⁵¹, M. Weirich⁹⁷, C. Weiser⁵⁰, P.S. Wells³⁵, T. Wenaus²⁹, T. Wengler³⁵, S. Wenig³⁵, N. Wermes²⁴, M.D. Werner⁷⁶, P. Werner³⁵, M. Wessels^{59a}, T.D. Weston²⁰, K. Whalen¹²⁸, N.L. Whallon¹⁴⁵, A.M. Wharton⁸⁷, A.S. White¹⁰³, A. White⁸, M.J. White¹, R. White^{144b}, D. Whiteson¹⁶⁸, B.W. Whitmore⁸⁷, F.J. Wickens¹⁴¹, W. Wiedenmann¹⁷⁸, M. Wielers¹⁴¹, C. Wiglesworth³⁹, L.A.M. Wiik-Fuchs⁵⁰, A. Wildauer¹¹³, F. Wilk⁹⁸, H.G. Wilkens³⁵, L.J. Wilkins⁹¹, H.H. Williams¹³⁴, S. Williams³¹, C. Willis¹⁰⁴, S. Willocq¹⁰⁰, J.A. Wilson²¹, I. Wingerter-Seez⁵, E. Winkels¹⁵³, F. Winklmeier¹²⁸, O.J. Winston¹⁵³, B.T. Winter²⁴, M. Wittgen¹⁵⁰, M. Wobisch⁹³, A. Wolf⁹⁷, T.M.H. Wolf¹¹⁸, R. Wolff⁹⁹, M.W. Wolter⁸², H. Wolters^{137a,137c}, V.W.S. Wong¹⁷², N.L. Woods¹⁴³, S.D. Worm²¹, B.K. Wosiek⁸², K.W. Woźniak⁸², K. Wraight⁵⁵, M. Wu³⁶, S.L. Wu¹⁷⁸, X. Wu⁵², Y. Wu^{58a}, T.R. Wyatt⁹⁸, B.M. Wynne⁴⁸, S. Xella³⁹, Z. Xi¹⁰³, L. Xia¹⁷⁵, D. Xu^{15a}, H. Xu^{58a,e}, L. Xu²⁹, T. Xu¹⁴², W. Xu¹⁰³, B. Yabsley¹⁵⁴, S. Yacooob^{32a}, K. Yajima¹³⁰, D.P. Yallup⁹², D. Yamaguchi¹⁶², Y. Yamaguchi¹⁶², A. Yamamoto⁷⁹, T. Yamanaka¹⁶⁰, F. Yamane⁸⁰, M. Yamatani¹⁶⁰, T. Yamazaki¹⁶⁰, Y. Yamazaki⁸⁰, Z. Yan²⁵, H.J. Yang^{58c,58d}, H.T. Yang¹⁸, S. Yang⁷⁵, Y. Yang¹⁶⁰, Z. Yang¹⁷, W.-M. Yao¹⁸, Y.C. Yap⁴⁴, Y. Yasu⁷⁹, E. Yatsenko^{58c,58d}, J. Ye⁴¹, S. Ye²⁹, I. Yeletsikh⁷⁷, E. Yigitbasi²⁵, E. Yildirim⁹⁷, K. Yorita¹⁷⁶, K. Yoshihara¹³⁴, C.J.S. Young³⁵, C. Young¹⁵⁰, J. Yu⁸, J. Yu⁷⁶, X. Yue^{59a}, S.P.Y. Yuen²⁴, B. Zabinski⁸², G. Zacharis¹⁰, E. Zaffaroni⁵², R. Zaidan¹⁴, A.M. Zaitsev^{121,am}, N. Zakharchuk⁴⁴, J. Zalieckas¹⁷, S. Zambito⁵⁷, D. Zanzi³⁵, D.R. Zaripovas⁵⁵, S.V. Zeiřner⁴⁵, C. Zeitnitz¹⁷⁹, G. Zemaityte¹³², J.C. Zeng¹⁷⁰, Q. Zeng¹⁵⁰, O. Zenin¹²¹, D. Zerwas¹²⁹, M. Zgubič¹³², D.F. Zhang^{58b}, D. Zhang¹⁰³, F. Zhang¹⁷⁸, G. Zhang^{58a}, H. Zhang^{15c}, J. Zhang⁶, L. Zhang^{15c}, L. Zhang^{58a}, M. Zhang¹⁷⁰, P. Zhang^{15c}, R. Zhang^{58a}, R. Zhang²⁴, X. Zhang^{58b}, Y. Zhang^{15d}, Z. Zhang¹²⁹, P. Zhao⁴⁷, X. Zhao⁴¹, Y. Zhao^{58b,129,ai}, Z. Zhao^{58a}, A. Zhemchugov⁷⁷, B. Zhou¹⁰³, C. Zhou¹⁷⁸, L. Zhou⁴¹, M.S. Zhou^{15d}, M. Zhou¹⁵², N. Zhou^{58c}, Y. Zhou⁷, C.G. Zhu^{58b}, H.L. Zhu^{58a}, H. Zhu^{15a}, J. Zhu¹⁰³, Y. Zhu^{58a}, X. Zhuang^{15a}, K. Zhukov¹⁰⁸, V. Zhulanov^{120b,120a}, A. Zibell¹⁷⁴, D. Zieminska⁶³, N.I. Zimine⁷⁷, S. Zimmermann⁵⁰, Z. Zinonos¹¹³, M. Zinser⁹⁷, M. Ziolkowski¹⁴⁸, G. Zobernig¹⁷⁸, A. Zoccoli^{23b,23a}, K. Zoch⁵¹, T.G. Zorbas¹⁴⁶, R. Zou³⁶, M. Zur Nedden¹⁹, L. Zwalinski³⁵

¹ Department of Physics, University of Adelaide, Adelaide, Australia² Physics Department, SUNY Albany, Albany, NY, United States of America³ Department of Physics, University of Alberta, Edmonton, AB, Canada⁴ (a) Department of Physics, Ankara University, Ankara; (b) Istanbul Aydin University, Istanbul; (c) Division of Physics, TOBB University of Economics and Technology, Ankara, Turkey⁵ LAPP, Université Grenoble Alpes, Université Savoie Mont Blanc, CNRS/IN2P3, Annecy, France⁶ High Energy Physics Division, Argonne National Laboratory, Argonne, IL, United States of America⁷ Department of Physics, University of Arizona, Tucson, AZ, United States of America⁸ Department of Physics, University of Texas at Arlington, Arlington, TX, United States of America⁹ Physics Department, National and Kapodistrian University of Athens, Athens, Greece¹⁰ Physics Department, National Technical University of Athens, Zografou, Greece¹¹ Department of Physics, University of Texas at Austin, Austin, TX, United States of America¹² (a) Bahcesehir University, Faculty of Engineering and Natural Sciences, Istanbul; (b) Istanbul Bilgi University, Faculty of Engineering and Natural Sciences, Istanbul; (c) Department of Physics, Bogazici University, Istanbul; (d) Department of Physics Engineering, Gaziantep University, Gaziantep, Turkey¹³ Institute of Physics, Azerbaijan Academy of Sciences, Baku, Azerbaijan¹⁴ Institut de Física d'Altes Energies (IFAE), Barcelona Institute of Science and Technology, Barcelona, Spain¹⁵ (a) Institute of High Energy Physics, Chinese Academy of Sciences, Beijing; (b) Physics Department, Tsinghua University, Beijing; (c) Department of Physics, Nanjing University, Nanjing;¹⁶ (d) University of Chinese Academy of Science (UCAS), Beijing, China

- ¹⁶ Institute of Physics, University of Belgrade, Belgrade, Serbia
- ¹⁷ Department for Physics and Technology, University of Bergen, Bergen, Norway
- ¹⁸ Physics Division, Lawrence Berkeley National Laboratory and University of California, Berkeley, CA, United States of America
- ¹⁹ Institut für Physik, Humboldt Universität zu Berlin, Berlin, Germany
- ²⁰ Albert Einstein Center for Fundamental Physics and Laboratory for High Energy Physics, University of Bern, Bern, Switzerland
- ²¹ School of Physics and Astronomy, University of Birmingham, Birmingham, United Kingdom
- ²² Centro de Investigaciones, Universidad Antonio Nariño, Bogota, Colombia
- ²³ (a) Dipartimento di Fisica e Astronomia, Università di Bologna, Bologna; (b) INFN Sezione di Bologna, Italy
- ²⁴ Physikalisches Institut, Universität Bonn, Bonn, Germany
- ²⁵ Department of Physics, Boston University, Boston, MA, United States of America
- ²⁶ Department of Physics, Brandeis University, Waltham, MA, United States of America
- ²⁷ (a) Transilvania University of Brasov, Brasov; (b) Horia Hulubei National Institute of Physics and Nuclear Engineering, Bucharest; (c) Department of Physics, Alexandru Ioan Cuza University of Iasi, Iasi; (d) National Institute for Research and Development of Isotopic and Molecular Technologies, Physics Department, Cluj-Napoca; (e) University Politehnica Bucharest, Bucharest; (f) West University in Timisoara, Timisoara, Romania
- ²⁸ (a) Faculty of Mathematics, Physics and Informatics, Comenius University, Bratislava; (b) Department of Subnuclear Physics, Institute of Experimental Physics of the Slovak Academy of Sciences, Kosice, Slovak Republic
- ²⁹ Physics Department, Brookhaven National Laboratory, Upton, NY, United States of America
- ³⁰ Departamento de Física, Universidad de Buenos Aires, Buenos Aires, Argentina
- ³¹ Cavendish Laboratory, University of Cambridge, Cambridge, United Kingdom
- ³² (a) Department of Physics, University of Cape Town, Cape Town; (b) Department of Mechanical Engineering Science, University of Johannesburg, Johannesburg; (c) School of Physics, University of the Witwatersrand, Johannesburg, South Africa
- ³³ Department of Physics, Carleton University, Ottawa, ON, Canada
- ³⁴ (a) Faculté des Sciences Ain Chock, Réseau Universitaire de Physique des Hautes Energies – Université Hassan II, Casablanca; (b) Centre National de l’Energie des Sciences Techniques Nucleaires (CNESTEN), Rabat; (c) Faculté des Sciences Semlalia, Université Cadi Ayyad, LPHEA, Marrakech; (d) Faculté des Sciences, Université Mohamed Premier and LPTPM, Oujda; (e) Faculté des sciences, Université Mohammed V, Rabat, Morocco
- ³⁵ CERN, Geneva, Switzerland
- ³⁶ Enrico Fermi Institute, University of Chicago, Chicago, IL, United States of America
- ³⁷ LPC, Université Clermont Auvergne, CNRS/IN2P3, Clermont-Ferrand, France
- ³⁸ Nevis Laboratory, Columbia University, Irvington, NY, United States of America
- ³⁹ Niels Bohr Institute, University of Copenhagen, Copenhagen, Denmark
- ⁴⁰ (a) Dipartimento di Fisica, Università della Calabria, Rende; (b) INFN Gruppo Collegato di Cosenza, Laboratori Nazionali di Frascati, Italy
- ⁴¹ Physics Department, Southern Methodist University, Dallas, TX, United States of America
- ⁴² Physics Department, University of Texas at Dallas, Richardson, TX, United States of America
- ⁴³ (a) Department of Physics, Stockholm University; (b) Oskar Klein Centre, Stockholm, Sweden
- ⁴⁴ Deutsches Elektronen-Synchrotron DESY, Hamburg and Zeuthen, Germany
- ⁴⁵ Lehrstuhl für Experimentelle Physik IV, Technische Universität Dortmund, Dortmund, Germany
- ⁴⁶ Institut für Kern- und Teilchenphysik, Technische Universität Dresden, Dresden, Germany
- ⁴⁷ Department of Physics, Duke University, Durham, NC, United States of America
- ⁴⁸ SUPA – School of Physics and Astronomy, University of Edinburgh, Edinburgh, United Kingdom
- ⁴⁹ INFN e Laboratori Nazionali di Frascati, Frascati, Italy
- ⁵⁰ Physikalisches Institut, Albert-Ludwigs-Universität Freiburg, Freiburg, Germany
- ⁵¹ II. Physikalisches Institut, Georg-August-Universität Göttingen, Göttingen, Germany
- ⁵² Département de Physique Nucléaire et Corpusculaire, Université de Genève, Genève, Switzerland
- ⁵³ (a) Dipartimento di Fisica, Università di Genova, Genova; (b) INFN Sezione di Genova, Italy
- ⁵⁴ II. Physikalisches Institut, Justus-Liebig-Universität Giessen, Giessen, Germany
- ⁵⁵ SUPA – School of Physics and Astronomy, University of Glasgow, Glasgow, United Kingdom
- ⁵⁶ LPSC, Université Grenoble Alpes, CNRS/IN2P3, Grenoble INP, Grenoble, France
- ⁵⁷ Laboratory for Particle Physics and Cosmology, Harvard University, Cambridge, MA, United States of America
- ⁵⁸ (a) Department of Modern Physics and State Key Laboratory of Particle Detection and Electronics, University of Science and Technology of China, Hefei; (b) Institute of Frontier and Interdisciplinary Science and Key Laboratory of Particle Physics and Particle Irradiation (MOE), Shandong University, Qingdao; (c) School of Physics and Astronomy, Shanghai Jiao Tong University, KLPPAC-MoE, SKLPPC, Shanghai; (d) Tsung-Dao Lee Institute, Shanghai, China
- ⁵⁹ (a) Kirchhoff-Institut für Physik, Ruprecht-Karls-Universität Heidelberg, Heidelberg; (b) Physikalisches Institut, Ruprecht-Karls-Universität Heidelberg, Heidelberg, Germany
- ⁶⁰ Faculty of Applied Information Science, Hiroshima Institute of Technology, Hiroshima, Japan
- ⁶¹ (a) Department of Physics, Chinese University of Hong Kong, Shatin, N.T., Hong Kong; (b) Department of Physics, University of Hong Kong, Hong Kong; (c) Department of Physics and Institute for Advanced Study, Hong Kong University of Science and Technology, Clear Water Bay, Kowloon, Hong Kong, China
- ⁶² Department of Physics, National Tsing Hua University, Hsinchu, Taiwan
- ⁶³ Department of Physics, Indiana University, Bloomington, IN, United States of America
- ⁶⁴ (a) INFN Gruppo Collegato di Udine, Sezione di Trieste, Udine; (b) ICTP, Trieste; (c) Dipartimento di Chimica, Fisica e Ambiente, Università di Udine, Udine, Italy
- ⁶⁵ (a) INFN Sezione di Lecce; (b) Dipartimento di Matematica e Fisica, Università del Salento, Lecce, Italy
- ⁶⁶ (a) INFN Sezione di Milano; (b) Dipartimento di Fisica, Università di Milano, Milano, Italy
- ⁶⁷ (a) INFN Sezione di Napoli; (b) Dipartimento di Fisica, Università di Napoli, Napoli, Italy
- ⁶⁸ (a) INFN Sezione di Pavia; (b) Dipartimento di Fisica, Università di Pavia, Pavia, Italy
- ⁶⁹ (a) INFN Sezione di Pisa; (b) Dipartimento di Fisica E. Fermi, Università di Pisa, Pisa, Italy
- ⁷⁰ (a) INFN Sezione di Roma; (b) Dipartimento di Fisica, Sapienza Università di Roma, Roma, Italy
- ⁷¹ (a) INFN Sezione di Roma Tor Vergata; (b) Dipartimento di Fisica, Università di Roma Tor Vergata, Roma, Italy
- ⁷² (a) INFN Sezione di Roma Tre; (b) Dipartimento di Matematica e Fisica, Università Roma Tre, Roma, Italy
- ⁷³ (a) INFN-TIFPA; (b) Università degli Studi di Trento, Trento, Italy
- ⁷⁴ Institut für Astro- und Teilchenphysik, Leopold-Franzens-Universität, Innsbruck, Austria
- ⁷⁵ University of Iowa, Iowa City, IA, United States of America
- ⁷⁶ Department of Physics and Astronomy, Iowa State University, Ames, IA, United States of America
- ⁷⁷ Joint Institute for Nuclear Research, Dubna, Russia
- ⁷⁸ (a) Departamento de Engenharia Elétrica, Universidade Federal de Juiz de Fora (UFJF), Juiz de Fora; (b) Universidade Federal do Rio De Janeiro COPPE/EE/IF, Rio de Janeiro; (c) Universidade Federal de São João del Rei (UFSJ), São João del Rei; (d) Instituto de Física, Universidade de São Paulo, São Paulo, Brazil
- ⁷⁹ KEK, High Energy Accelerator Research Organization, Tsukuba, Japan
- ⁸⁰ Graduate School of Science, Kobe University, Kobe, Japan
- ⁸¹ (a) AGH University of Science and Technology, Faculty of Physics and Applied Computer Science, Krakow; (b) Marian Smoluchowski Institute of Physics, Jagiellonian University, Krakow, Poland
- ⁸² Institute of Nuclear Physics Polish Academy of Sciences, Krakow, Poland
- ⁸³ Faculty of Science, Kyoto University, Kyoto, Japan
- ⁸⁴ Kyoto University of Education, Kyoto, Japan

- 85 Research Center for Advanced Particle Physics and Department of Physics, Kyushu University, Fukuoka, Japan
- 86 Instituto de Física La Plata, Universidad Nacional de La Plata and CONICET, La Plata, Argentina
- 87 Physics Department, Lancaster University, Lancaster, United Kingdom
- 88 Oliver Lodge Laboratory, University of Liverpool, Liverpool, United Kingdom
- 89 Department of Experimental Particle Physics, Jožef Stefan Institute and Department of Physics, University of Ljubljana, Ljubljana, Slovenia
- 90 School of Physics and Astronomy, Queen Mary University of London, London, United Kingdom
- 91 Department of Physics, Royal Holloway University of London, Egham, United Kingdom
- 92 Department of Physics and Astronomy, University College London, London, United Kingdom
- 93 Louisiana Tech University, Ruston, LA, United States of America
- 94 Fysiska institutionen, Lunds universitet, Lund, Sweden
- 95 Centre de Calcul de l'Institut National de Physique Nucléaire et de Physique des Particules (IN2P3), Villeurbanne, France
- 96 Departamento de Física Teórica C-15 and CIAFF, Universidad Autónoma de Madrid, Madrid, Spain
- 97 Institut für Physik, Universität Mainz, Mainz, Germany
- 98 School of Physics and Astronomy, University of Manchester, Manchester, United Kingdom
- 99 CPPM, Aix-Marseille Université, CNRS/IN2P3, Marseille, France
- 100 Department of Physics, University of Massachusetts, Amherst, MA, United States of America
- 101 Department of Physics, McGill University, Montreal, QC, Canada
- 102 School of Physics, University of Melbourne, Victoria, Australia
- 103 Department of Physics, University of Michigan, Ann Arbor, MI, United States of America
- 104 Department of Physics and Astronomy, Michigan State University, East Lansing, MI, United States of America
- 105 B.I. Stepanov Institute of Physics, National Academy of Sciences of Belarus, Minsk, Belarus
- 106 Research Institute for Nuclear Problems of Byelorussian State University, Minsk, Belarus
- 107 Group of Particle Physics, University of Montreal, Montreal, QC, Canada
- 108 P.N. Lebedev Physical Institute of the Russian Academy of Sciences, Moscow, Russia
- 109 Institute for Theoretical and Experimental Physics (ITEP), Moscow, Russia
- 110 National Research Nuclear University MEPhI, Moscow, Russia
- 111 D.V. Skobeltsyn Institute of Nuclear Physics, M.V. Lomonosov Moscow State University, Moscow, Russia
- 112 Fakultät für Physik, Ludwig-Maximilians-Universität München, München, Germany
- 113 Max-Planck-Institut für Physik (Werner-Heisenberg-Institut), München, Germany
- 114 Nagasaki Institute of Applied Science, Nagasaki, Japan
- 115 Graduate School of Science and Kobayashi-Maskawa Institute, Nagoya University, Nagoya, Japan
- 116 Department of Physics and Astronomy, University of New Mexico, Albuquerque, NM, United States of America
- 117 Institute for Mathematics, Astrophysics and Particle Physics, Radboud University Nijmegen/Nikhef, Nijmegen, Netherlands
- 118 Nikhef National Institute for Subatomic Physics and University of Amsterdam, Amsterdam, Netherlands
- 119 Department of Physics, Northern Illinois University, DeKalb, IL, United States of America
- 120 ^(a) Budker Institute of Nuclear Physics, SB RAS, Novosibirsk; ^(b) Novosibirsk State University Novosibirsk, Russia
- 121 Institute for High Energy Physics of the National Research Centre Kurchatov Institute, Protvino, Russia
- 122 Department of Physics, New York University, New York, NY, United States of America
- 123 Ohio State University, Columbus, OH, United States of America
- 124 Faculty of Science, Okayama University, Okayama, Japan
- 125 Homer L. Dodge Department of Physics and Astronomy, University of Oklahoma, Norman, OK, United States of America
- 126 Department of Physics, Oklahoma State University, Stillwater, OK, United States of America
- 127 Palacký University, RCPTM, Joint Laboratory of Optics, Olomouc, Czech Republic
- 128 Center for High Energy Physics, University of Oregon, Eugene, OR, United States of America
- 129 LAL, Université Paris-Sud, CNRS/IN2P3, Université Paris-Saclay, Orsay, France
- 130 Graduate School of Science, Osaka University, Osaka, Japan
- 131 Department of Physics, University of Oslo, Oslo, Norway
- 132 Department of Physics, Oxford University, Oxford, United Kingdom
- 133 LPNHE, Sorbonne Université, Paris Diderot Sorbonne Paris Cité, CNRS/IN2P3, Paris, France
- 134 Department of Physics, University of Pennsylvania, Philadelphia, PA, United States of America
- 135 Konstantinov Nuclear Physics Institute of National Research Centre "Kurchatov Institute", PNPI, St. Petersburg, Russia
- 136 Department of Physics and Astronomy, University of Pittsburgh, Pittsburgh, PA, United States of America
- 137 ^(a) Laboratório de Instrumentação e Física Experimental de Partículas – LIP; ^(b) Departamento de Física, Faculdade de Ciências, Universidade de Lisboa, Lisboa; ^(c) Departamento de Física, Universidade de Coimbra, Coimbra; ^(d) Centro de Física Nuclear da Universidade de Lisboa, Lisboa; ^(e) Departamento de Física, Universidade do Minho, Braga; ^(f) Departamento de Física Teórica y del Cosmos, Universidad de Granada, Granada (Spain); ^(g) Dep Física and CEFITEC de Faculdade de Ciências e Tecnologia, Universidade Nova de Lisboa, Caparica, Portugal
- 138 Institute of Physics, Academy of Sciences of the Czech Republic, Prague, Czech Republic
- 139 Czech Technical University in Prague, Prague, Czech Republic
- 140 Charles University, Faculty of Mathematics and Physics, Prague, Czech Republic
- 141 Particle Physics Department, Rutherford Appleton Laboratory, Didcot, United Kingdom
- 142 IRFU, CEA, Université Paris-Saclay, Gif-sur-Yvette, France
- 143 Santa Cruz Institute for Particle Physics, University of California Santa Cruz, Santa Cruz, CA, United States of America
- 144 ^(a) Departamento de Física, Pontificia Universidad Católica de Chile, Santiago; ^(b) Departamento de Física, Universidad Técnica Federico Santa María, Valparaíso, Chile
- 145 Department of Physics, University of Washington, Seattle, WA, United States of America
- 146 Department of Physics and Astronomy, University of Sheffield, Sheffield, United Kingdom
- 147 Department of Physics, Shinshu University, Nagano, Japan
- 148 Department Physik, Universität Siegen, Siegen, Germany
- 149 Department of Physics, Simon Fraser University, Burnaby, BC, Canada
- 150 SLAC National Accelerator Laboratory, Stanford, CA, United States of America
- 151 Physics Department, Royal Institute of Technology, Stockholm, Sweden
- 152 Departments of Physics and Astronomy, Stony Brook University, Stony Brook, NY, United States of America
- 153 Department of Physics and Astronomy, University of Sussex, Brighton, United Kingdom
- 154 School of Physics, University of Sydney, Sydney, Australia
- 155 Institute of Physics, Academia Sinica, Taipei, Taiwan
- 156 ^(a) E. Andronikashvili Institute of Physics, Iv. Javakhishvili Tbilisi State University, Tbilisi; ^(b) High Energy Physics Institute, Tbilisi State University, Tbilisi, Georgia
- 157 Department of Physics, Technion, Israel Institute of Technology, Haifa, Israel
- 158 Raymond and Beverly Sackler School of Physics and Astronomy, Tel Aviv University, Tel Aviv, Israel
- 159 Department of Physics, Aristotle University of Thessaloniki, Thessaloniki, Greece
- 160 International Center for Elementary Particle Physics and Department of Physics, University of Tokyo, Tokyo, Japan
- 161 Graduate School of Science and Technology, Tokyo Metropolitan University, Tokyo, Japan
- 162 Department of Physics, Tokyo Institute of Technology, Tokyo, Japan

- ¹⁶³ Tomsk State University, Tomsk, Russia
¹⁶⁴ Department of Physics, University of Toronto, Toronto, ON, Canada
¹⁶⁵ ^(a) TRIUMF, Vancouver, BC; ^(b) Department of Physics and Astronomy, York University, Toronto, ON, Canada
¹⁶⁶ Division of Physics and Tomonaga Center for the History of the Universe, Faculty of Pure and Applied Sciences, University of Tsukuba, Tsukuba, Japan
¹⁶⁷ Department of Physics and Astronomy, Tufts University, Medford, MA, United States of America
¹⁶⁸ Department of Physics and Astronomy, University of California Irvine, Irvine, CA, United States of America
¹⁶⁹ Department of Physics and Astronomy, University of Uppsala, Uppsala, Sweden
¹⁷⁰ Department of Physics, University of Illinois, Urbana, IL, United States of America
¹⁷¹ Instituto de Física Corpuscular (IFIC), Centro Mixto Universidad de Valencia – CSIC, Valencia, Spain
¹⁷² Department of Physics, University of British Columbia, Vancouver, BC, Canada
¹⁷³ Department of Physics and Astronomy, University of Victoria, Victoria, BC, Canada
¹⁷⁴ Fakultät für Physik und Astronomie, Julius-Maximilians-Universität Würzburg, Würzburg, Germany
¹⁷⁵ Department of Physics, University of Warwick, Coventry, United Kingdom
¹⁷⁶ Waseda University, Tokyo, Japan
¹⁷⁷ Department of Particle Physics, Weizmann Institute of Science, Rehovot, Israel
¹⁷⁸ Department of Physics, University of Wisconsin, Madison, WI, United States of America
¹⁷⁹ Fakultät für Mathematik und Naturwissenschaften, Fachgruppe Physik, Bergische Universität Wuppertal, Wuppertal, Germany
¹⁸⁰ Department of Physics, Yale University, New Haven, CT, United States of America
¹⁸¹ Yerevan Physics Institute, Yerevan, Armenia

^a Also at Borough of Manhattan Community College, City University of New York, NY; United States of America.

^b Also at California State University, East Bay; United States of America.

^c Also at Centre for High Performance Computing, CSIR Campus, Rosebank, Cape Town; South Africa.

^d Also at CERN, Geneva; Switzerland.

^e Also at CPPM, Aix-Marseille Université, CNRS/IN2P3, Marseille; France.

^f Also at Département de Physique Nucléaire et Corpusculaire, Université de Genève, Genève; Switzerland.

^g Also at Departament de Física de la Universitat Autònoma de Barcelona, Barcelona; Spain.

^h Also at Departamento de Física Teórica y del Cosmos, Universidad de Granada, Granada (Spain); Spain.

ⁱ Also at Department of Applied Physics and Astronomy, University of Sharjah, Sharjah; United Arab Emirates.

^j Also at Department of Financial and Management Engineering, University of the Aegean, Chios; Greece.

^k Also at Department of Physics and Astronomy, University of Louisville, Louisville, KY; United States of America.

^l Also at Department of Physics and Astronomy, University of Sheffield, Sheffield; United Kingdom.

^m Also at Department of Physics, California State University, Fresno CA; United States of America.

ⁿ Also at Department of Physics, California State University, Sacramento CA; United States of America.

^o Also at Department of Physics, King's College London, London; United Kingdom.

^p Also at Department of Physics, St. Petersburg State Polytechnical University, St. Petersburg; Russia.

^q Also at Department of Physics, Stanford University; United States of America.

^r Also at Department of Physics, University of Fribourg, Fribourg; Switzerland.

^s Also at Department of Physics, University of Michigan, Ann Arbor MI; United States of America.

^t Also at Dipartimento di Fisica E. Fermi, Università di Pisa, Pisa; Italy.

^u Also at Giresun University, Faculty of Engineering, Giresun; Turkey.

^v Also at Graduate School of Science, Osaka University, Osaka; Japan.

^w Also at Hellenic Open University, Patras; Greece.

^x Also at Horia Hulubei National Institute of Physics and Nuclear Engineering, Bucharest; Romania.

^y Also at II. Physikalisches Institut, Georg-August-Universität Göttingen, Göttingen; Germany.

^z Also at Institutio Catalana de Recerca i Estudis Avancats, ICREA, Barcelona; Spain.

^{aa} Also at Institut für Experimentalphysik, Universität Hamburg, Hamburg; Germany.

^{ab} Also at Institute for Mathematics, Astrophysics and Particle Physics, Radboud University Nijmegen/Nikhef, Nijmegen; Netherlands.

^{ac} Also at Institute for Particle and Nuclear Physics, Wigner Research Centre for Physics, Budapest; Hungary.

^{ad} Also at Institute of Particle Physics (IPP); Canada.

^{ae} Also at Institute of Physics, Academia Sinica, Taipei; Taiwan.

^{af} Also at Institute of Physics, Azerbaijan Academy of Sciences, Baku; Azerbaijan.

^{ag} Also at Institute of Theoretical Physics, Ilia State University, Tbilisi; Georgia.

^{ah} Also at Istanbul University, Dept. of Physics, Istanbul; Turkey.

^{ai} Also at LAL, Université Paris-Sud, CNRS/IN2P3, Université Paris-Saclay, Orsay; France.

^{aj} Also at Louisiana Tech University, Ruston LA; United States of America.

^{ak} Also at LPNHE, Sorbonne Université, Paris Diderot Sorbonne Paris Cité, CNRS/IN2P3, Paris; France.

^{al} Also at Manhattan College, New York NY; United States of America.

^{am} Also at Moscow Institute of Physics and Technology State University, Dolgoprudny; Russia.

^{an} Also at National Research Nuclear University MEPhI, Moscow; Russia.

^{ao} Also at Near East University, Nicosia, North Cyprus, Mersin; Turkey.

^{ap} Also at Physikalisches Institut, Albert-Ludwigs-Universität Freiburg, Freiburg; Germany.

^{aq} Also at School of Physics, Sun Yat-sen University, Guangzhou; China.

^{ar} Also at The City College of New York, New York NY; United States of America.

^{as} Also at The Collaborative Innovation Center of Quantum Matter (CICQM), Beijing; China.

^{at} Also at Tomsk State University, Tomsk, and Moscow Institute of Physics and Technology State University, Dolgoprudny; Russia.

^{au} Also at TRIUMF, Vancouver BC; Canada.

^{av} Also at Università di Napoli Parthenope, Napoli; Italy.

* Deceased.